PACIFIC EARTHQUAKE ENGINEERING RESEARCH CENTER

Hanging-Wall Scaling using Finite-Fault Simulations

Jennifer L. Donahue
Geosyntec Consultants

Norman A. Abrahamson
Department of Civil and Environmental Engineering
University of California, Berkeley

PEER 2013/14
SEPTEMBER 2013

Hanging-Wall Scaling using Finite-Fault Simulations

Jennifer L. Donahue
Geosyntec Consultants

Norman A. Abrahamson
Department of Civil and Environmental Engineering
University of California, Berkeley

PEER Report 2013/14
Pacific Earthquake Engineering Research Center
Headquarters at the University of California, Berkeley

September 2013

ABSTRACT

The hanging-wall (HW) effect is defined as the increase in ground motions observed during a reverse earthquake event, when in close proximity and while on the hanging-wall side of a fault. As observed in the empirical data, the short period ground motions over the hanging-wall may be twice the amplitude of the ground motions recorded on the footwall at the same rupture distance. Because there are only a few earthquakes with near-fault recordings, there is insufficient empirical data to constrain the dependence of the HW effect. Using finite-fault simulations, 34 reverse earthquake events were simulated. The scenarios varied the magnitude between M6 and M7.8, dips from 20 to 70 degrees, and distances to top of rupture of 0 and 5 km.

A simplified parametric model for the median hanging-wall effect was developed using the distance parameters R_x and R_y, magnitude, fault dip, fault width, and depth to top of rupture. The HW effect reaches it maximum over the bottom edge of the rupture. The residuals for the model fall within the range -0.2 to 0.2 natural log units. The scaling constraints derived in this study are being used in part or in whole in many of the NGA-West2 GMPEs and lead to more consistent HW effects.

ACKNOWLEDGMENTS

The NGA-West2 research program was sponsored by the Pacific Earthquake Engineering Research Center (PEER) and funded by the California Earthquake Authority, California Department of Transportation, and the Pacific Gas & Electric Company (PG&E). Any opinions, findings, and conclusions or recommendations expressed in this material are those of the authors and do not necessarily reflect those of the sponsoring agencies. Additional support was provided by PG&E.

CONTENTS

LIST OF FIGURES

LIST OF TABLES

LIST OF APPENDICES

1 Introduction

The hanging-wall (HW) effect is defined as the increase in ground motions observed for sites located in close proximity to the rupture plane and on the HW as compared to sites located on the footwall (FW). As observed in the empirical data, the short-period ground motions may be a factor of 2–3 larger over the HW, but are not well constrained by the sparse available empirical data.

1.1 REVIEW OF PREVIOUS HANGING WALL MODELS: ABRAHAMSON AND SOMERVILLE (1996)

Following the 1994 Northridge, California, earthquake, Abrahamson and Somerville [1996] found that recordings on the HW side of the fault typically exhibited greater than average ground motions when compared to recordings at the same distance on the FW side. Using this information, they derived an empirical model for the HW effect that results in a 50% increase in peak horizontal accelerations over the HW, which attenuated with distance. From these findings, they postulated that ground motions for other reverse events would also lead to similar systematic increases.

1.2 REVIEW OF PREVIOUS HANGING-WALL MODELS: NGA (2008)

In 2008, as part of the Next Generation Attenuation (NGA) project, coordinated by the Pacific Earthquake Engineering Research Center (PEER), five ground motion prediction equations (GMPEs) were developed to model ground motion for shallow crustal earthquakes in the western United States. Three of these models incorporated a term for the HW effect: Abrahamson and Silva [2008]; Campbell and Bozorgnia [2008]; and Chiou and Youngs [2008]. The Boore and Atkinson [2008] model does not specifically include a HW term, but the effect of the HW is implicitly captured by the use of the R_{JB} distance metric as the primary distance scaling parameter. The Idriss model [2008], which uses a simple functional form, does not include a HW term, nor does it attempt to capture differences in the ground motion on the HW and FW sides of the rupture.

The HW effect mentioned in the three aforementioned models are dependent on different predictive parameters. Each of these HW models was developed utilizing the distance metric R_x, dip of the fault, and depth to top of rupture. However, the Abrahamson and Silva [2008] model is also dependent on the distance metrics R_x, fault width, and magnitude. The Campbell and

Bozorgnia [2008] model also relies on the distance metrics R_{RUP} and magnitude. The Chiou and Youngs, [2008] model represented the HW effect by using a combination of the distance metrics R_{JB} and R_{RUP}.

To properly constrain the HW effect, multiple recordings are needed from sites located on both the HW and FW sides of the rupture and at short distances. In NGA dataset [PEER 2005], only two earthquakes meet these criteria: the 1994 Northridge California, earthquake and 1999 Chi-Chi, Taiwan, earthquake. Based on this limited availability, the modelers made assumptions on the scaling of the HW effect for magnitude, distance, dip, and rupture depth. This lead to large differences between the different GMPEs, driven by different assumptions on the HW scaling that did not have a strong empirical constraint (e.g., scaling with magnitude, dip, and depth).

Figures 1.1 through 1.3 are the results for the five 2008 NGA models. Figure 1.1 illustrates differences in magnitude scaling, while Figure 1.2 illustrates comparisons for dip of the fault and Figure 1.3 for depth scaling. From Figure 1.1, it is apparent that magnitude scaling was not been well constrained. The Chiou and Youngs [2008] model, shown as the green line, has the largest HW factors, particularly at **M**6 and 6.5, culminating in the weakest magnitude scaling. At lower magnitudes, the effect of the HW tapers more quickly than the larger magnitudes, leading to the convergence of the GMPEs at different R_x distances. For instance at **M**6 and 6.5, the GMPEs reconverge near R_x = 25 km and 30 km, respectively. However, the **M** 7 and 7.5 GMPEs reconverge near an R_x distance of 40 km and greater. Figure 1.2 illustrates the lack of constraint on the effect of the dip of the fault. Because there is more empirical data available for steeply dipping faults, (e.g., 60º and 70º), the GMPEs are better constrained for steeply dipping ruptures than for shallow dipping ruptures, leading to large discrepancies in the GMPE results for shallow dips. More empirical data with HW effects are available for the shallow rupture depths than for deep rupture depths. As seen in Figure 1.3, as the depth to top of rupture increases, so does the differences in the both the FW and HW ground motions for the GMPEs.

As previously stated, one of the first events used to constrain the HW effect was the 1994 Northridge event. This **M**6.69 with a dip of 40º and a depth to top of rupture of 5 km was first used to constrain the magnitude scaling. Figure 1.4b for the Northridge event shows general agreement between the GMPEs both over the rupture plane and at greater distances; the exception in the Idriss model [2008] as it does not include a HW model. This agreement between the GMPEs is also consistent for the **M**6 scenario, but the GMPE results begin to diverge rapidly with greater magnitudes.

The 1999 Chi-Chi, Taiwan, event provided additional data on which to draw assumptions for the HW effect, especially for larger magnitude, shallow dipping events. Although Figure 1.5d for the Chi-Chi event shows a wide range between the GMPEs over the rupture plane, the Abrahamson and Silva [2008], Boore and Atkinson [2008], and Chiou and Youngs [2008] converge at an R_x distance of 30 km and beyond. Coincidently, there is empirical data at this distance from the fault that the developers used to constrain the effect. The Campbell and Bozorgnia [2008] model has much weaker HW factors for this event.

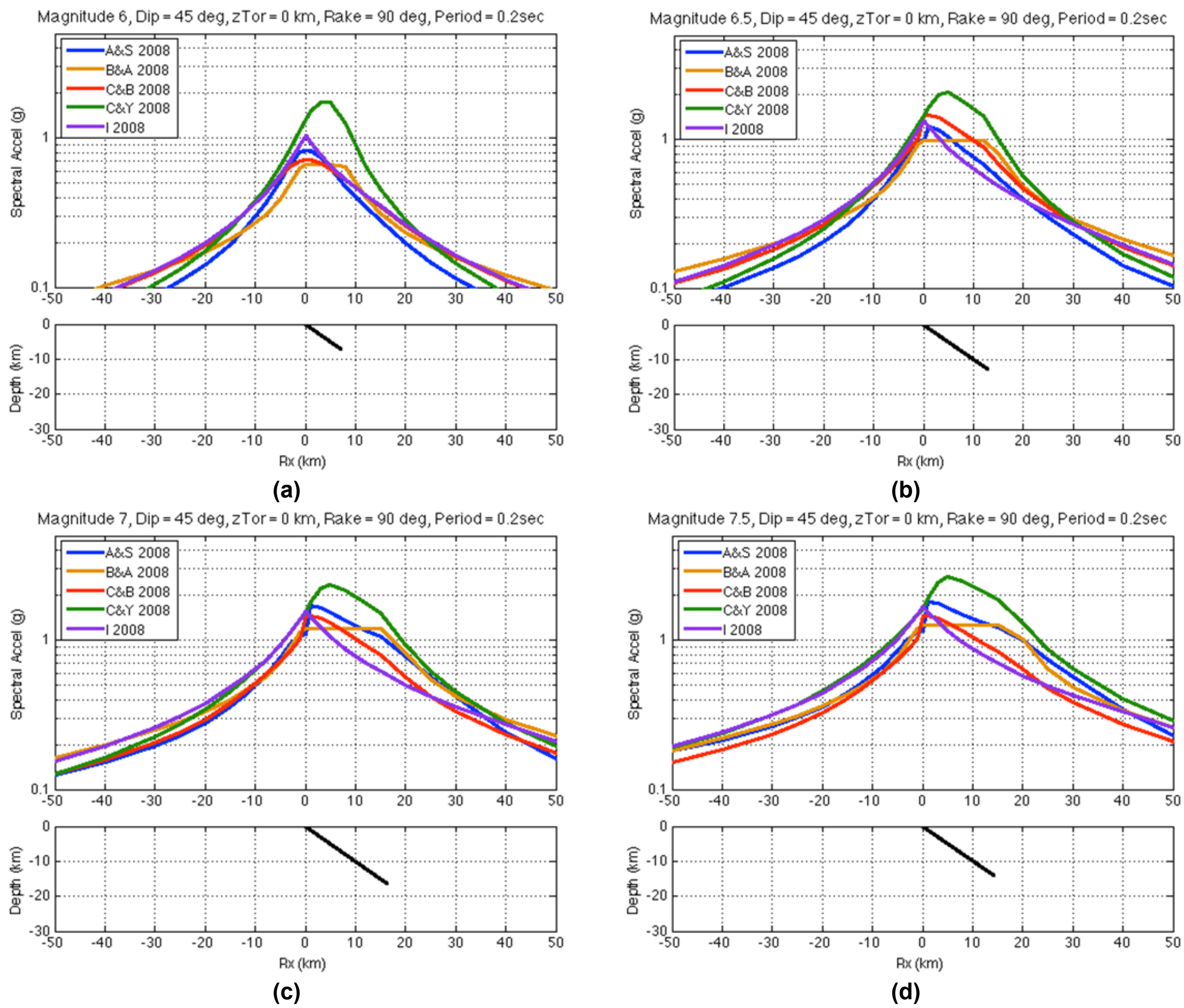

Figure 1.1 **Comparison of the hanging-wall results for five 2008 NGA models; shown here are surface ruptures with a dip of 45º with varied magnitudes: (a) M6, (b) M6.5, (c) M7, and (d) M7.5.**

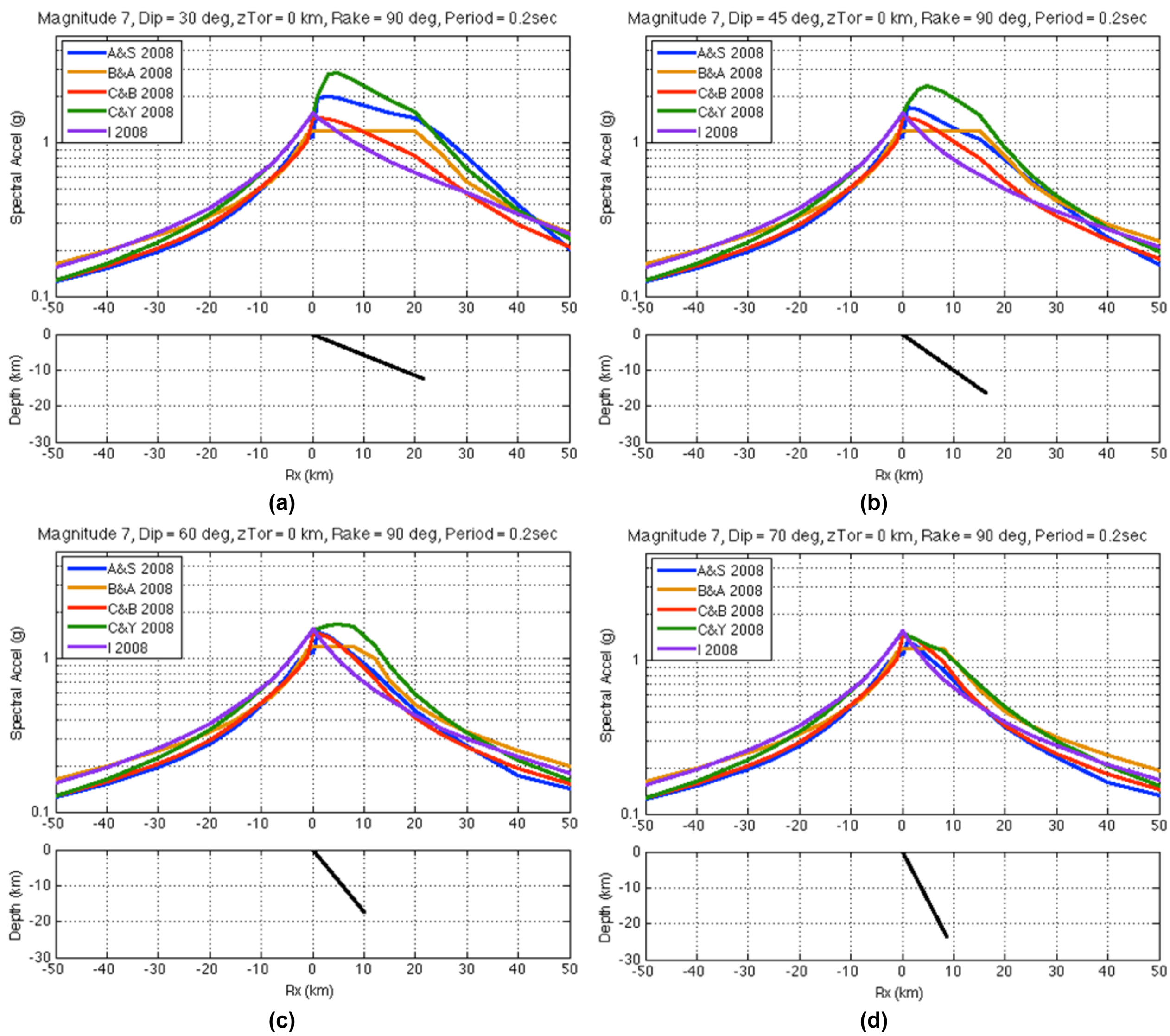

Figure 1.2 **Comparison of the hanging-wall results for the five 2008 NGA models ; shown here are M7 surface ruptures with varied dips: (a) 30º, (b) 45º, (c) 60º, and (d) 70º.**

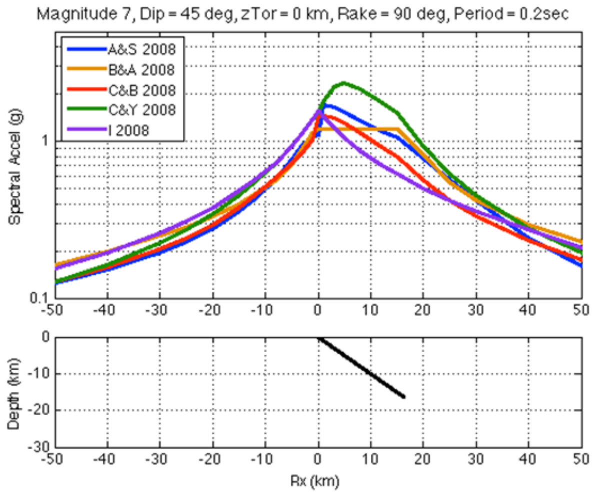

(a)

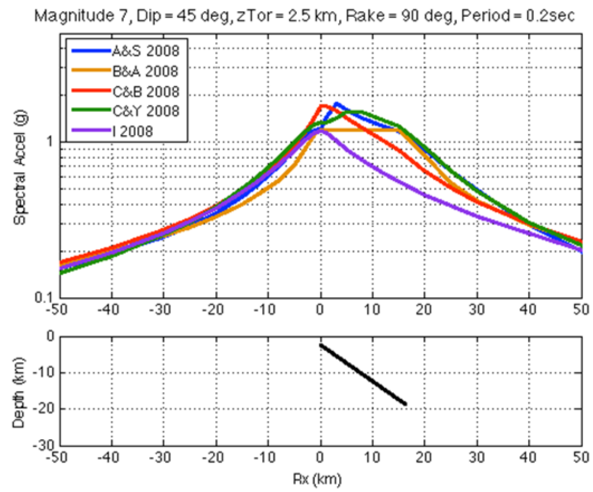

(b)

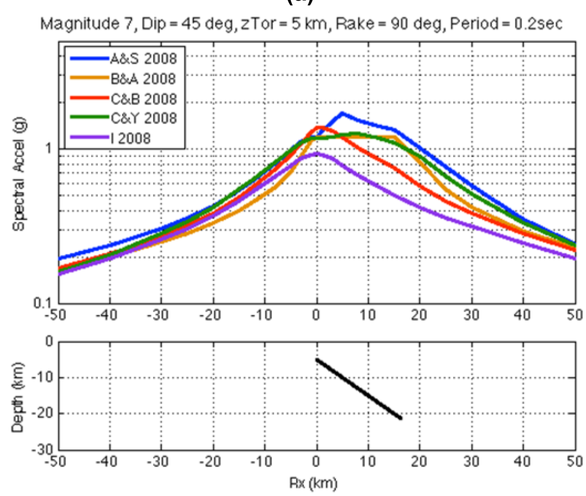

(c)

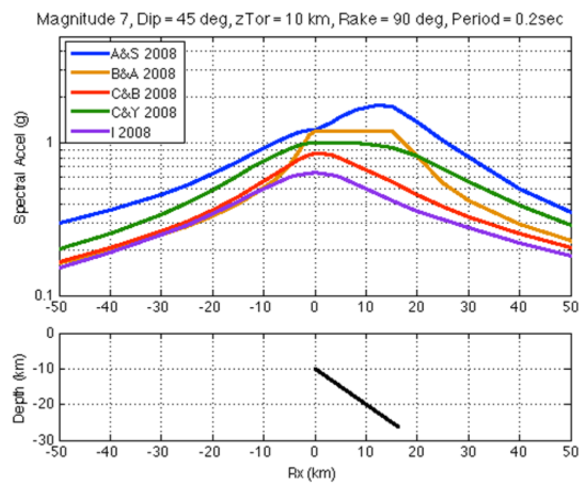

(d)

Figure 1.3 **Comparison of the hanging-wall results for five 2008 NGA models ; shown here are M7 events with a dip of 45º with varied depths: (a) 0 km, (b) 2.5 km, (c) 5 km, and (d) 10 km.**

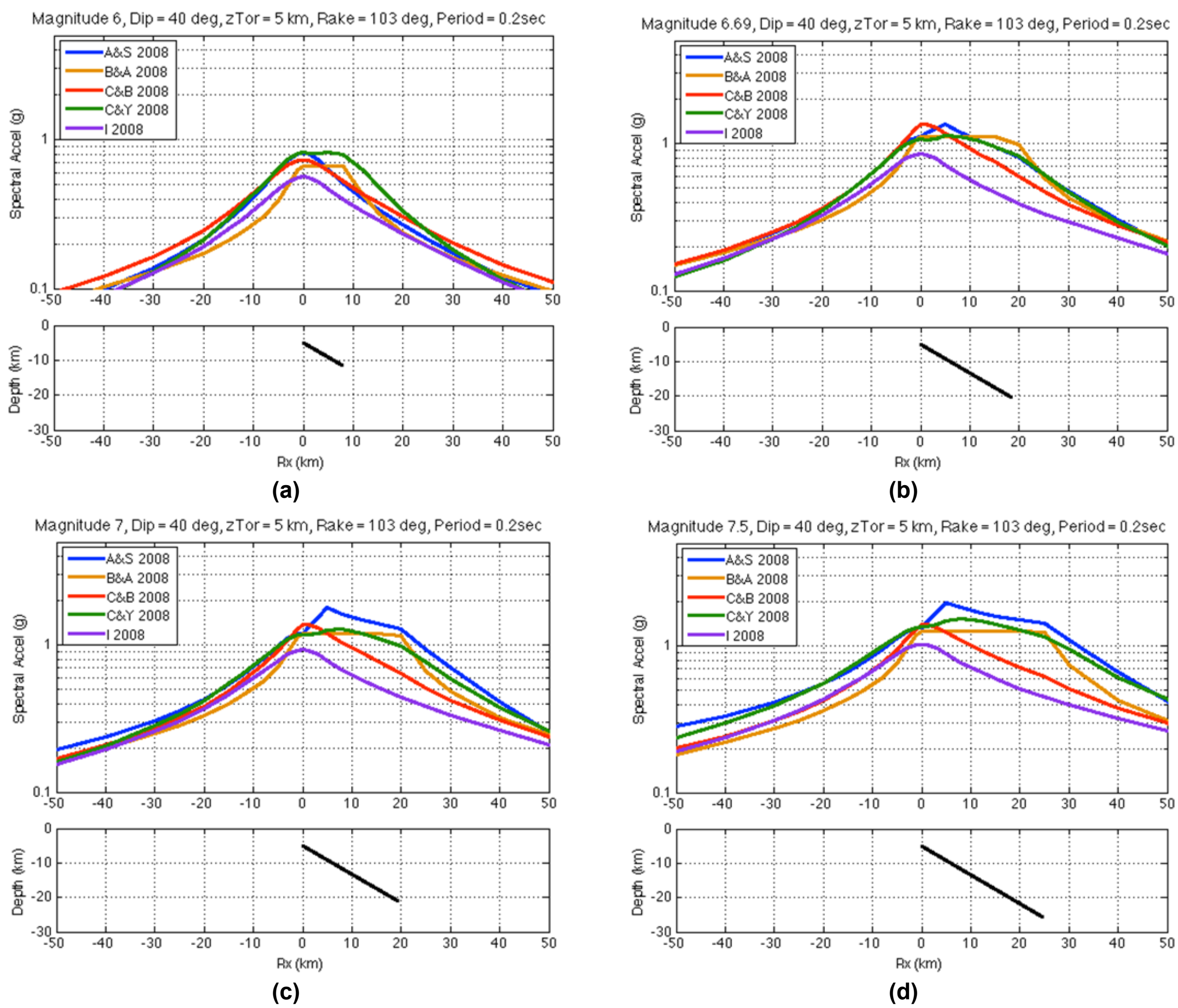

Figure 1.4 **The hanging-wall results for five 2008 NGA models using the 1994 Northridge earthquake as a comparison; shown here are buried ruptures with a dip of 40º, with varied magnitudes: (a) M6, (b) M6.69, (c) M7, and (d) M7.5.**

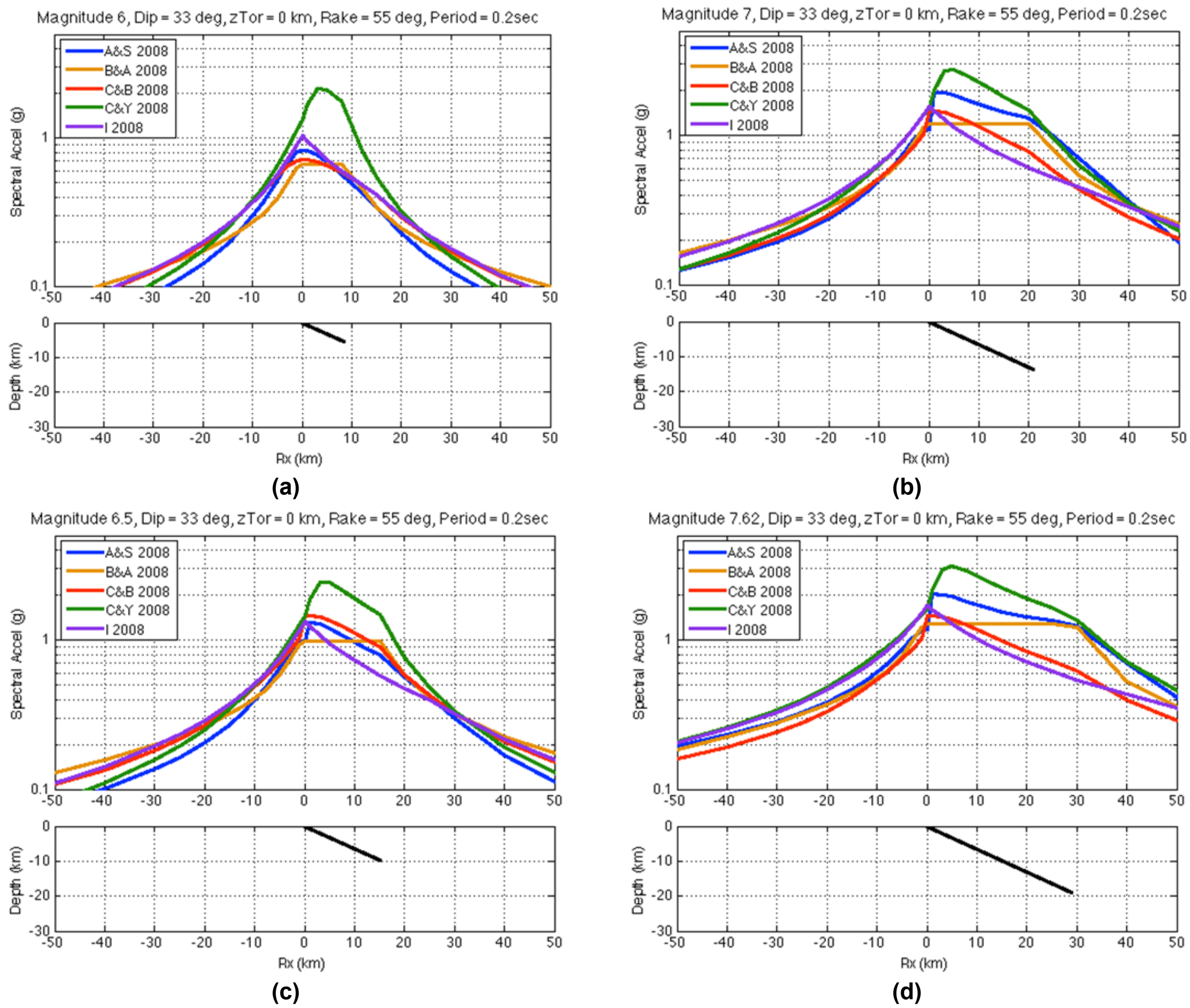

Figure 1.5 **The hanging-wall results for five 2008 NGA models using the 1999 Chi-Chi event as a comparison; shown here are surface ruptures with a dip of 33º, with varied magnitudes: (a) M6, (b) M6.5, (c) M7, and (d) M7.62.**

1.3 EMPIRICAL DATA IN NGA-WEST 2 DATABASE

As mentioned in the previous section, the PEER 2008 NGA database had only a few events with recordings on both the FW and HW sides of the rupture at short distances. With the completion of the NGA-West2 database, several additional events could be considered to constrain the HW effect. Table 1.1 shows the earthquakes with at least one recording on the HW and FW within a rupture distance of 15 km.

Of the events listed above, the Imperial Valley-06, Northridge-01, Chi-Chi Taiwan, L'Aquila Italy, and Wenchuan, China, have at least three recordings over the HW and stations at close distances on the FW. Figure 1.6 shows the total residuals comparing the recorded spectral accelerations against the 2008 Abrahamson and Silva model. . The total residuals for the Abrahamson and Silva [2008] and Chiou and Youngs [2008] models, with no HW effect term, are shown in Appendix A for all events in Table 1.1 with various periods.

Table 1.1 Listing of earthquakes in the 2008 NGA and 2013 NGA-West2 databases with at least five recordings within 80 km, and at least one recording on both the footwall and hanging-wall with R_{JB} distances of 15 km or less located along the rupture.

Database	Event	Year	Mag	Dip	No. of records	No. of records R_{JB}=0	No. of records < 15 km on footwall	No. of records < 15 km on hanging wall
NGA (2008)	Imperial Valley-06	1979	6.53	80	19	3	8	8
NGA (2008)	Irpinia, Italy-01	1980	6.9	60	5	0	1	1
NGA (2008)	Whittier Narrows-01	1987	5.99	30	13	1	5	6
NGA (2008)	Loma Prieta, CA	1989	6.93	70	14	1	3	6
NGA (2008)	Northridge-01	1994	6.69	40	26	10	3	12
NGA (2008)	Kobe, Japan	1995	6.9	85	14	1	8	1
NGA (2008)	Chi-Chi, Taiwan	1999	7.62	33	53	7	24	7
NGA (2008)	Chi-Chi, Taiwan-06	1999	6.3	30	34	1	2	1
NGA-W2	Niigata, Japan	2004	6.63	47	23	0	2	2
NGA-W2	L'Aquila, Italy	2009	6.3	48	7	4	2	4
NGA-W2	Wenchuan, China	2008	7.9	50	34	3	1	5
NGA-W2	Iwate	2008	6.9	40	37	1	2	3
NGA-W2	El Mayor-Cucapah	2010	7.2	63	9	0	1	1
NGA-W2	Darfield, New Zealand	2010	7	82.2	17	1	3	4
NGA-W2	Christchurch, New Zealand	2011	6.2	67	6	1	4	2

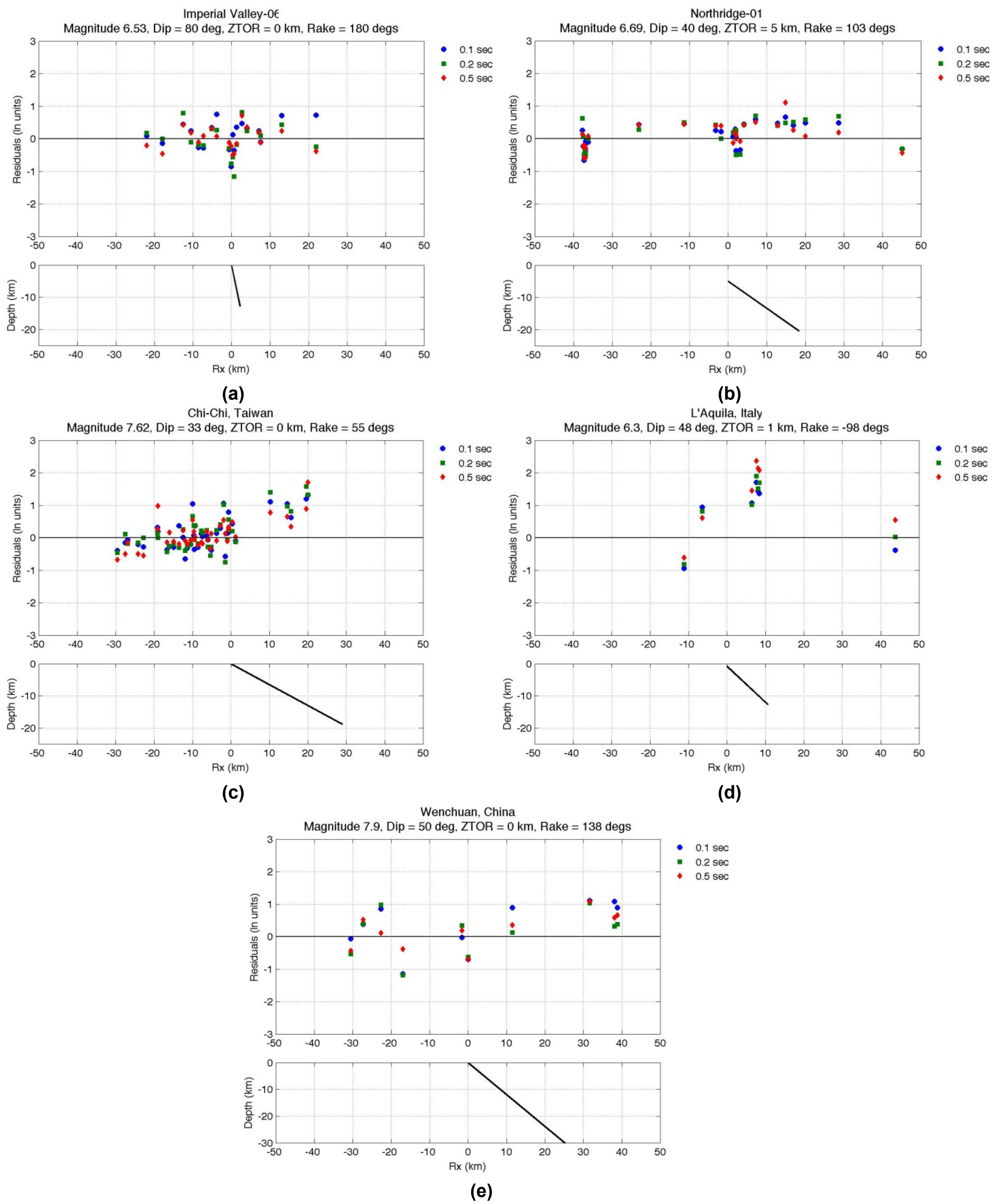

Figure 1.6 **Intra-event residuals (in natural log units) for selected events with at least five recordings within 80 km, and at least one recording on the footwall with R_{JB} distances of 15 km or less, and three or more recordings directly over the rupture plane: (a) Imperial Valley, (b) Northridge, (c) Chi-Chi, (d) L'Aquila, and e) Wenchuan.**

Using the subset of fifteen events in Table 1.1, correlations between magnitude, dip of the fault, and depth to top of rupture were investigated. As seen in Figure 1.7 below, there does not appear to be a trend with the magnitude of the event and the dip of the fault. In Figure 1.8, there does appear to be a correlation between the events with deep tops of ruptures and the magnitude: as the magnitude increases, the depth to top of rupture tends to decrease. The dip of the fault and the depth to top of rupture also appear to be correlated. The deeper events appear to occur with shallower dipping faults, as seen in Figure 1.9.

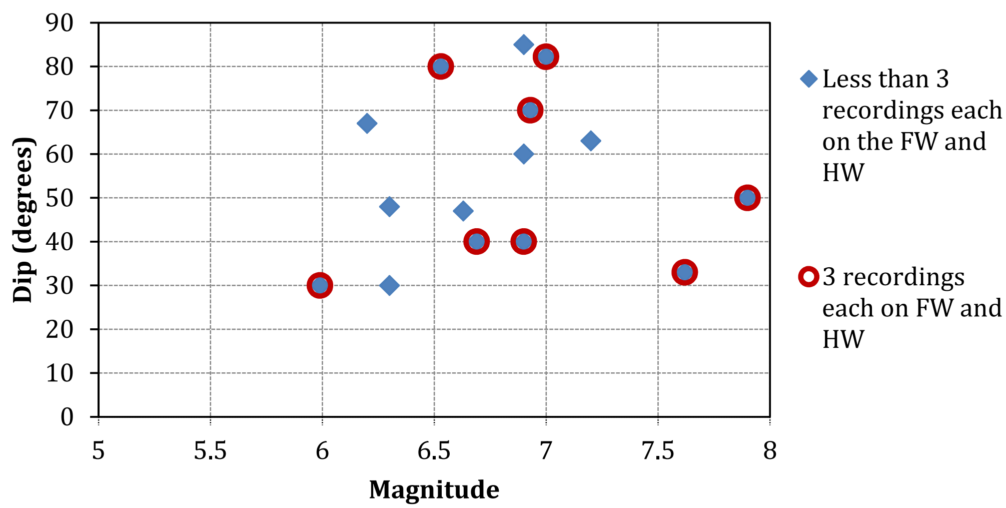

Figure 1.7 Comparison of magnitude and dip of the fault of events in Table 1.1.

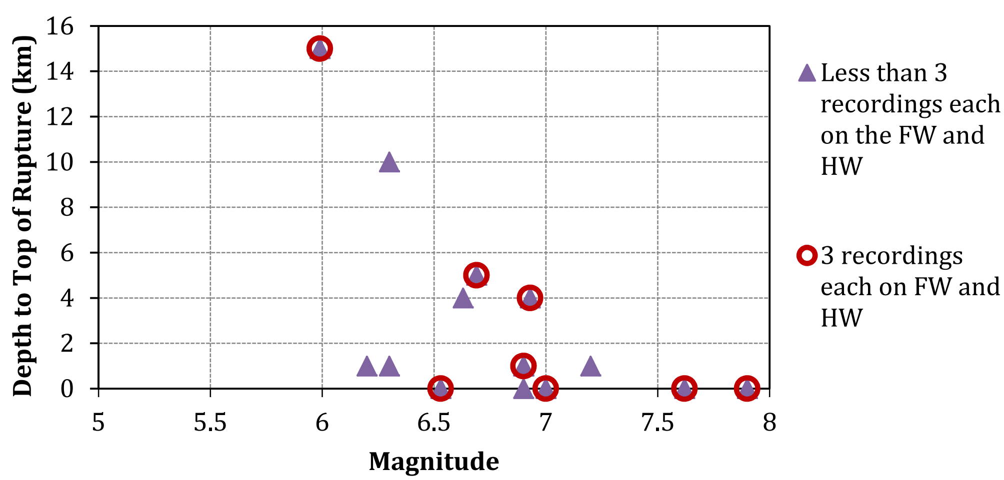

Figure 1.8 Comparison of magnitude and depth to top of rupture of the fault of events in Table 1.1

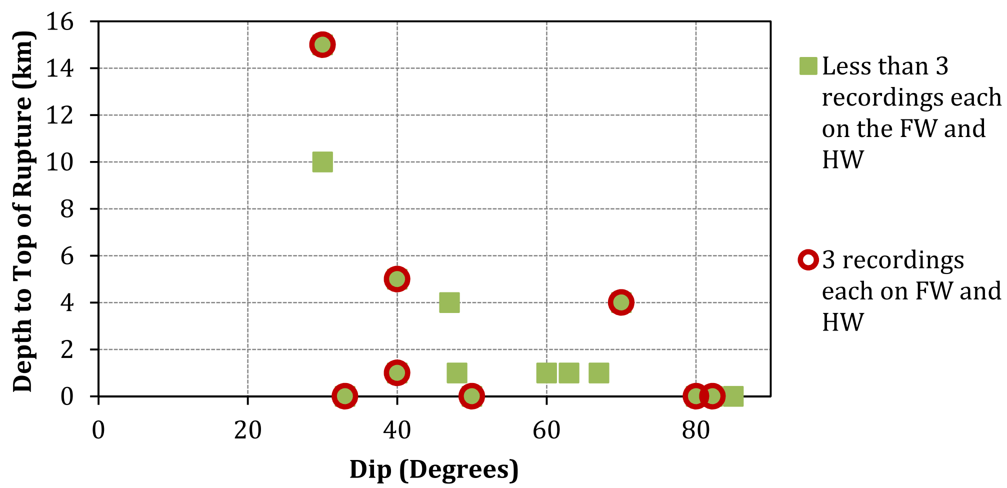

Figure 1.9 **Comparison of dip of the fault and depth to top of rupture of the fault of events in Table 1.1.**

2 Simulations Conducted

The sparse empirical data severely limits the ability to constraint the scaling of the HW effect based on distance, magnitude, dip, and rupture depth. For this reason, constraints on the HW scaling were developed using finite-fault simulations (FSS).

2.1 2004 RESULTS (PEA, UNR, URS)

As part of Working Group 4 for the 2008 PEER NGA project, rock ground motions were simulated for a suite of reverse slip events; see Table 2.1. In all, twelve scenarios were considered with magnitudes ranging from **M**6.5 to **M**7.8, dips ranging from 30–60°, and with surface and buried ruptures. For these reverse-slip simulations, the crustal thickness was assumed to be 20 km, and the velocity structure had a minimum of V_{s30} = 1800 m/sec.

Pacific Engineering and Analysis (PEA), the University of Reno (UNR), and URS Corporation undertook the simulations with varying results. A minimum of 20 realizations of slip distribution/ hypocenter combinations were needed. In almost all cases, the PEA model had higher resulting spectral accelerations, and the UNR model had lower spectral acceleration results. The results, mean, and standard deviation, of the simulations are presented in Figures 2.1 through 2.3.

From Figure 2.1, the effects of magnitude scaling for the hanging-wall effect are shown for a surface rupture with a constant dip for 45º. The three models are similar for the larger magnitudes and diverge as the magnitude decreases.

Table 2.1 Earthquake scenarios for PEA, UNR, and URS (2004) simulation runs.

Event Name	Magnitude	Area (km^2)	Width (km)	Length (km)	Dip	Top of Rupture (km)
RA	6.5	324	18	18	30	5
RB	6.5	324	18	18	45	0
RC	6.5	324	18	18	45	5
RD	6.5	324	18	18	45	10
RE	6.5	324	18	18	60	5
RF	7.0	1024	32	32	30	0
RG	7.0	1008	28	36	45	0
RH	7.0	1008	21	48	45	5
RI	7.0	989	23	43	60	0
RJ	7.5	3160	40	79	30	0
RK	7.5	3164	28	113	45	0
RL	7.8	6320	40	158	30	0

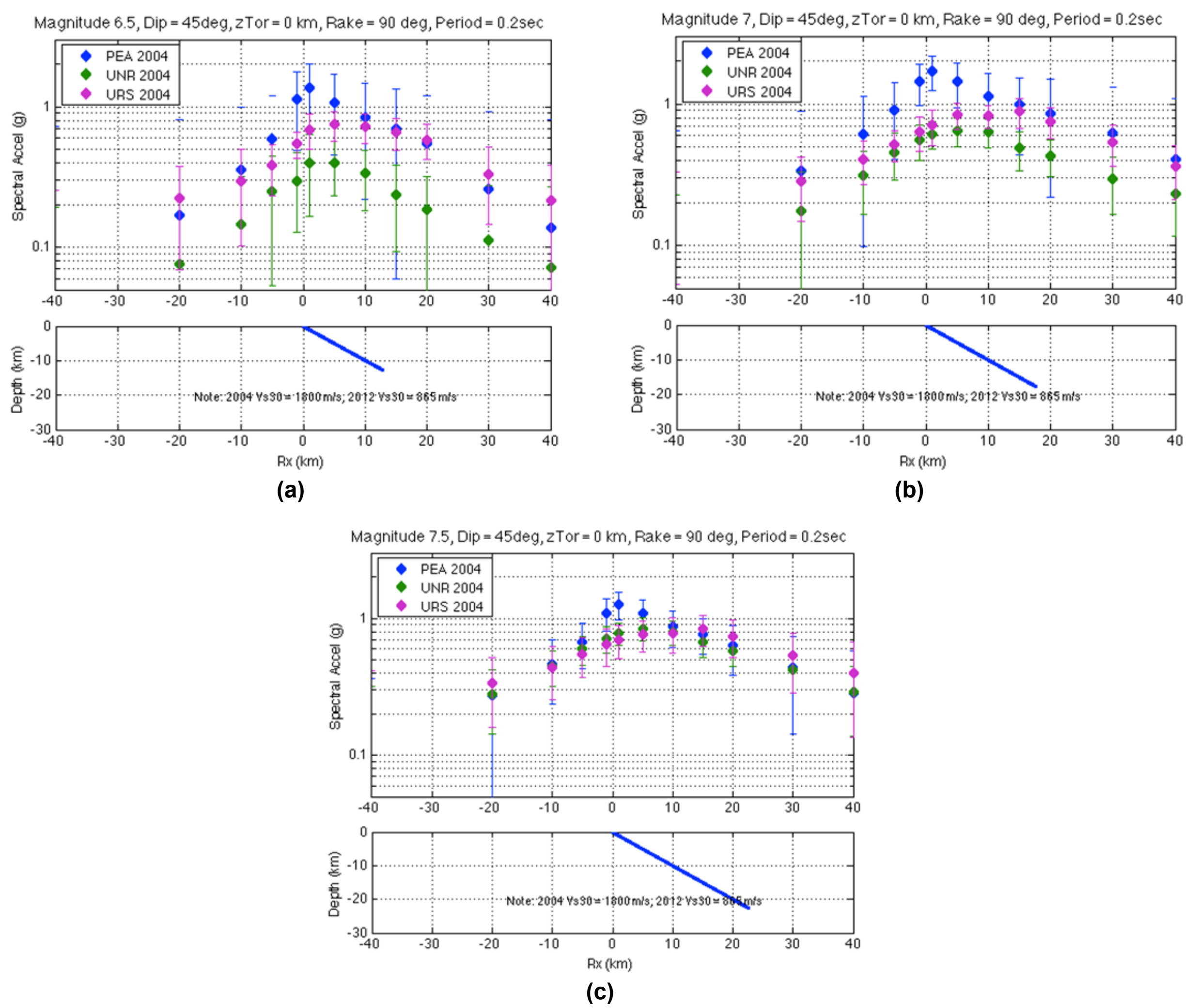

Figure 2.1 Comparison of the hanging-wall effects for the 2004 simulations; shown here are surface ruptures with a dip of 45º with varied magnitudes: (a) M6.5, (b) M7, and (c) M7.5.

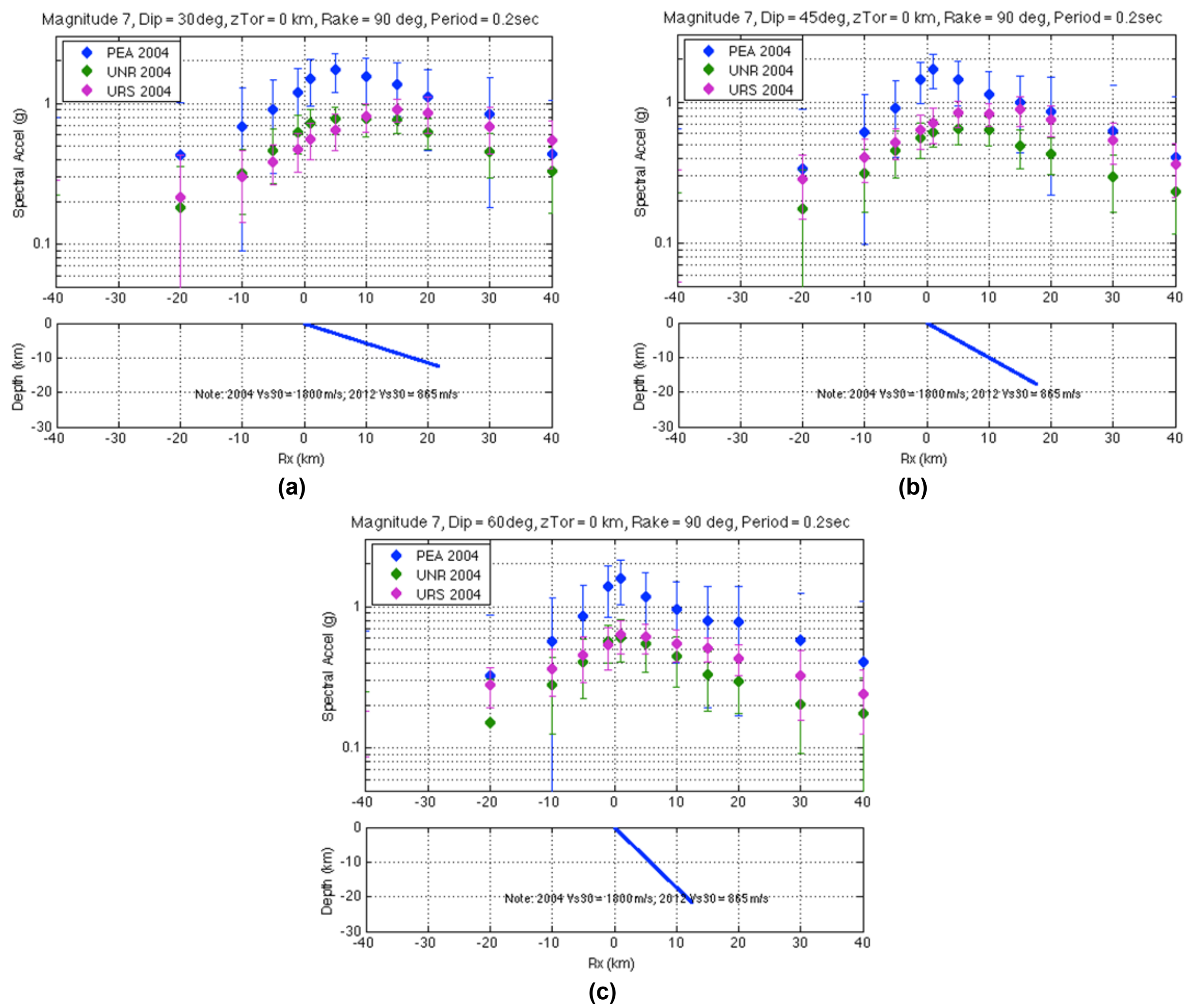

Figure 2.2 **Comparison of 2004 models; shown here are M7 surface ruptures with varied dips: (a) 30º, (b) 45º, and (c) 60º.**

In Figure 2.2, the effect of dip of the fault is compared. For these simulations, the results are fairly consistent between the three modelers, with larger HW effects for the shallower dips. Although the results for PEA shows a stronger HW effect than the other two models, the shape of the effect of dip on the HW is similar. Note that the effect of the HW extends further from the top of the rupture for shallower dips than for steeply dipping faults.

As shown in Figure 2.3, the three simulation results do not show similar HW effects for different rupture depths; however, the three sets of simulations show the same trend: that as the depth to the top of rupture increases, the effect of the HW tapers more slowly with distance.

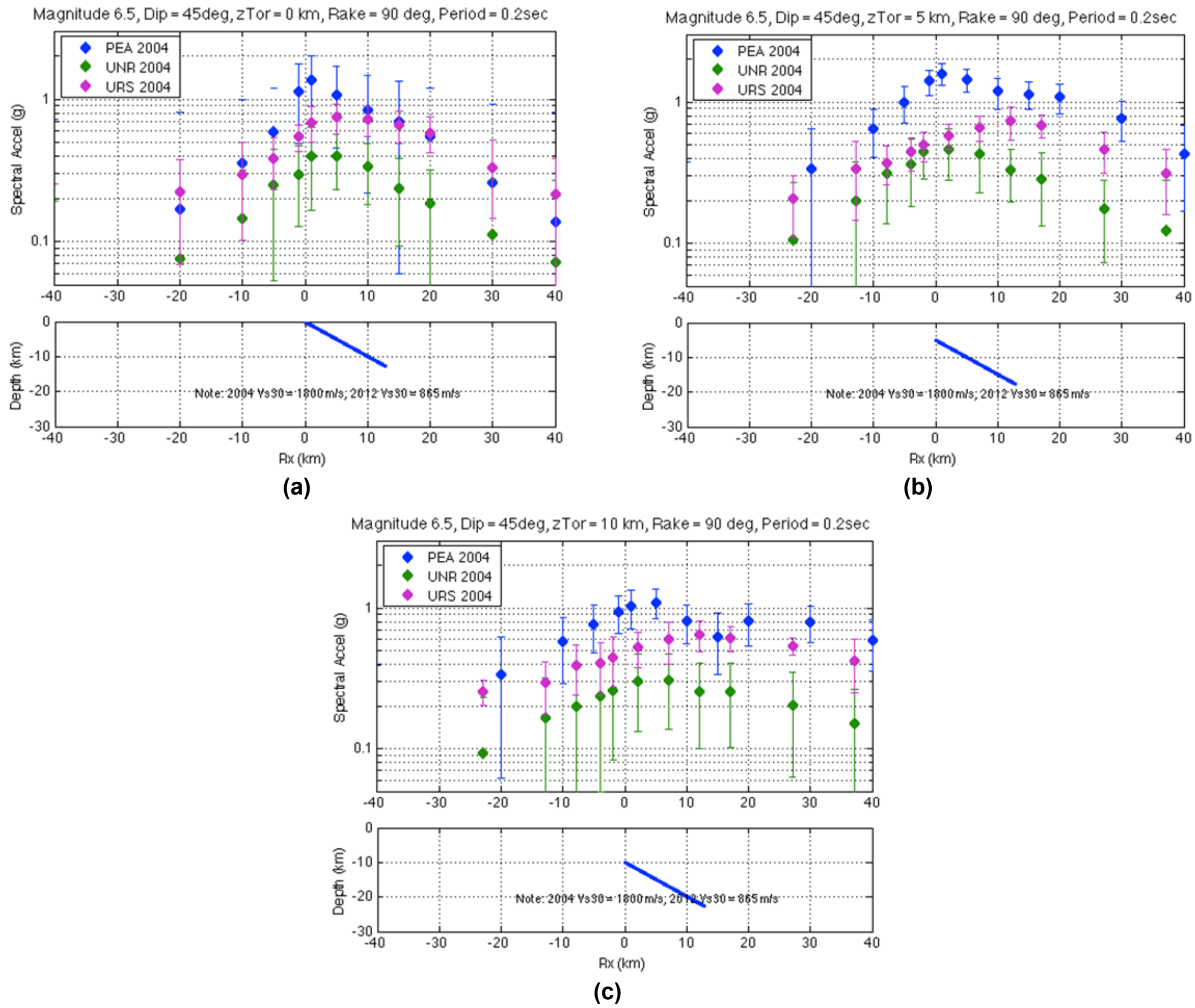

Figure 2.3 **Comparison of 2004 models; shown here are M6.5 with a dip of 45º with varied depths: (a) 0 km, (b) 5 km, and (c) 10 km.**

2.2 GRAVES AND PITARKA MODEL RESULTS

An additional set of FFS for HW effects were developed using the 2010 Graves and Pitarka [Graves and Pitarka, 2010] modules on the Southern California Earthquake Center (SCEC) broadband platform (BBP). Table 2.2 shows the 34 reverse earthquake events that were simulated. The scenarios varied the magnitude between **M**6 and **M**7.8, dips from 20–70°, distances to top of rupture of 0 and 5 km. The Graves and Pitarka (GP) model, developed for simulation of the Loma Prieta earthquake, uses a one-dimensional velocity model having a V_{s30} of 865 m/sec.

Table 2.2 Earthquake scenarios for GP model Set A and Set B simulation runs.

Magnitude	Area (km^2)	Width (km)	Length (km)	Dip	Top of Rupture (km)
6	100	10	10	20	0
6	100	10	10	30	0
6	100	10	10	45	0
6	100	10	10	60	0
6	100	10	10	70	0
6.5	324	18	18	20	0
6.5	324	18	18	30	0
6.5	324	18	18	45	0
6.5	324	18	18	60	0
6.5	324	18	18	70	0
7	1000	25	40	20	0
7	1000	25	40	30	0
7 *	1012	23	44	45	0
7	1000	25	40	45	0
7 *	1000	20	50	60	0
7	1000	25	40	60	0
7	1000	25	40	70	0
7.5	3200	32	100	20	0
7.5	3200	32	100	30	0
7.5*	3150	25	126	45	0
7.5	3200	32	100	45	0
7.5*	3000	20	150	60	0
7.5	3200	32	100	60	0
7.5	3200	32	100	70	0
7.8*	4500	25	180	45	0
7.8*	4500	20	200	60	0
6	100	10	10	20	5
6	100	10	10	30	5
6	100	10	10	45	5
6	100	10	10	60	5
6.5	324	18	18	20	5
6.5	324	18	18	30	5
6.5	324	18	18	45	5
6.5	324	18	18	60	5

(* Denotes GP Set B)

Originally, 28 scenarios were run; these are shown in Table 2.2, without an asterisk. For these original scenarios (GP Set A), the width and length were held constant for each magnitude. This assumption leads to some ruptures that may not be realistic: for scenarios with larger magnitudes and larger dip angles, the rupture extended below the traditional limit of the seismogenic depth. For this reason, four additional large magnitude scenarios were run that limited the width to be within the traditional seismogenic width and extended the length of the larger magnitudes, keeping the rupture area unchanged for the steeper dip angles. This ensured that at steeper dip angles, the bottom of the fault would not extend too deeply or past a reasonable seismogenic zone. Two additional **M**7.8 scenarios were also included in these latest runs. The GP Set B scenarios are marked in Table 2.2 with an asterisk. The GP Set A and Set B simulation results are compared to the HW effects from the 2004 simulations in Figures 2.4 through 2.6.

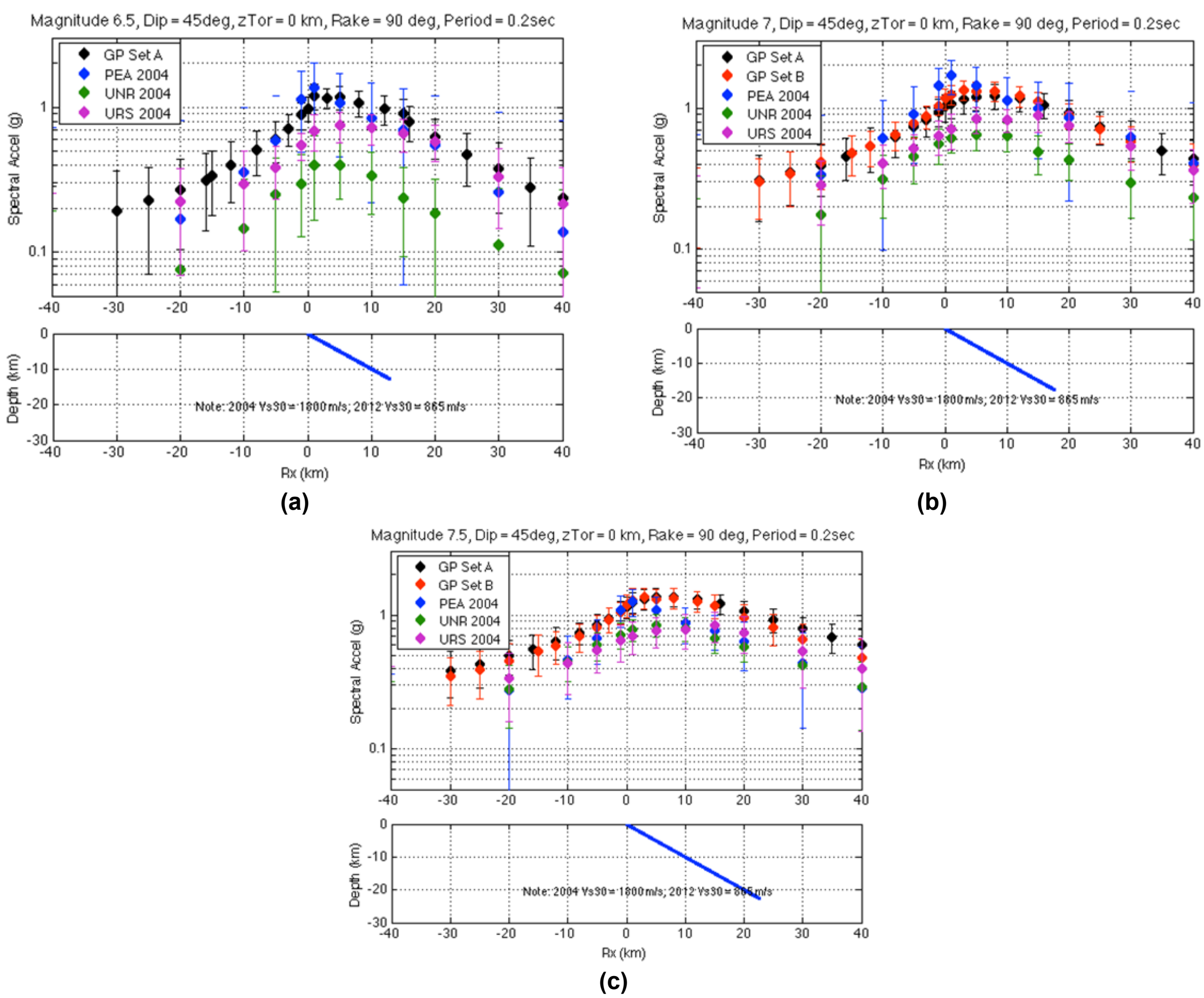

Figure 2.4 Comparison of 2004 and 2012 models; shown here are surface ruptures with a dip of 45º with varied magnitudes: (a) M6.5, (b) M7, and (c) M7.5.

From Figure 2.4, the GP Set A and Set B simulation results closely resemble each other and are within the same range of spectral acceleration as the 2004 PEA and 2004 URS models, despite the fact that the V_{s30} for the 2004 models is 1800 m/sec and the 2012 models' V_{s30} is 865 m/sec. In Figure 2.5, the GP Set A and Set B models are similar to those of the 2004 models and most closely resemble those of the PEA (2004) simulation results. Note that as the dip of the fault becomes steeper the FW and HW become more symmetric.

Figure 2.6 demonstrates the effect of the depth to the top of fault between the various simulations. Because the GP models did not simulate a depth to top of rupture below 5 km, it is not shown in Figure 2.6c. Here the GP Set A model closely follows the results of the 2004 PEA model on FW and the 2004 URS model. Also note in Figure 2.6b, the HW effects for the buried rupture from the GP Set A model are less than those of the GP Set A model in Figure 2.6a.

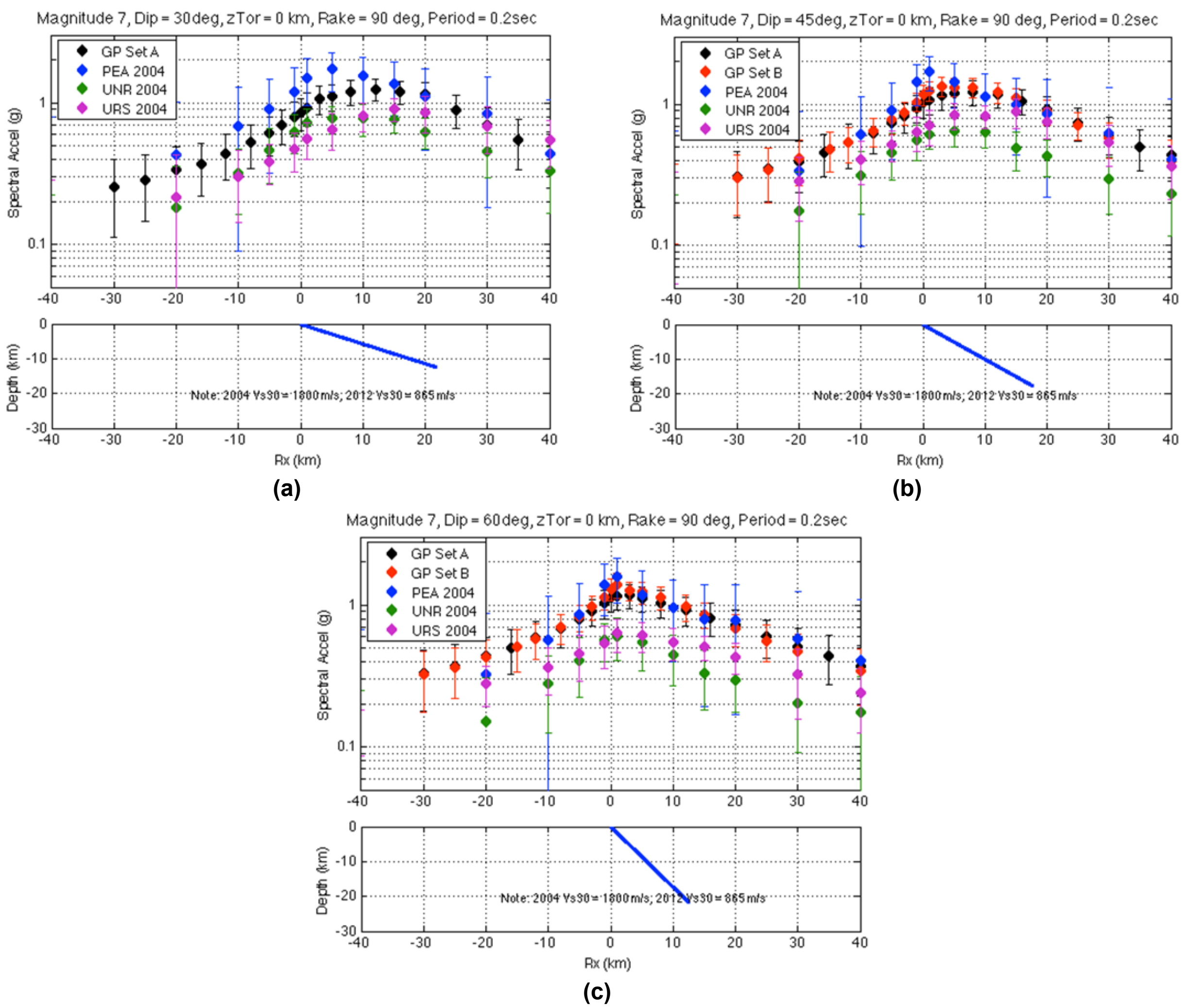

Figure 2.5 **Comparison of 2004 and 2012 models; shown here are M7 surface ruptures with varied dips: (a) 30º, (b) 45º, and (c) 60º.**

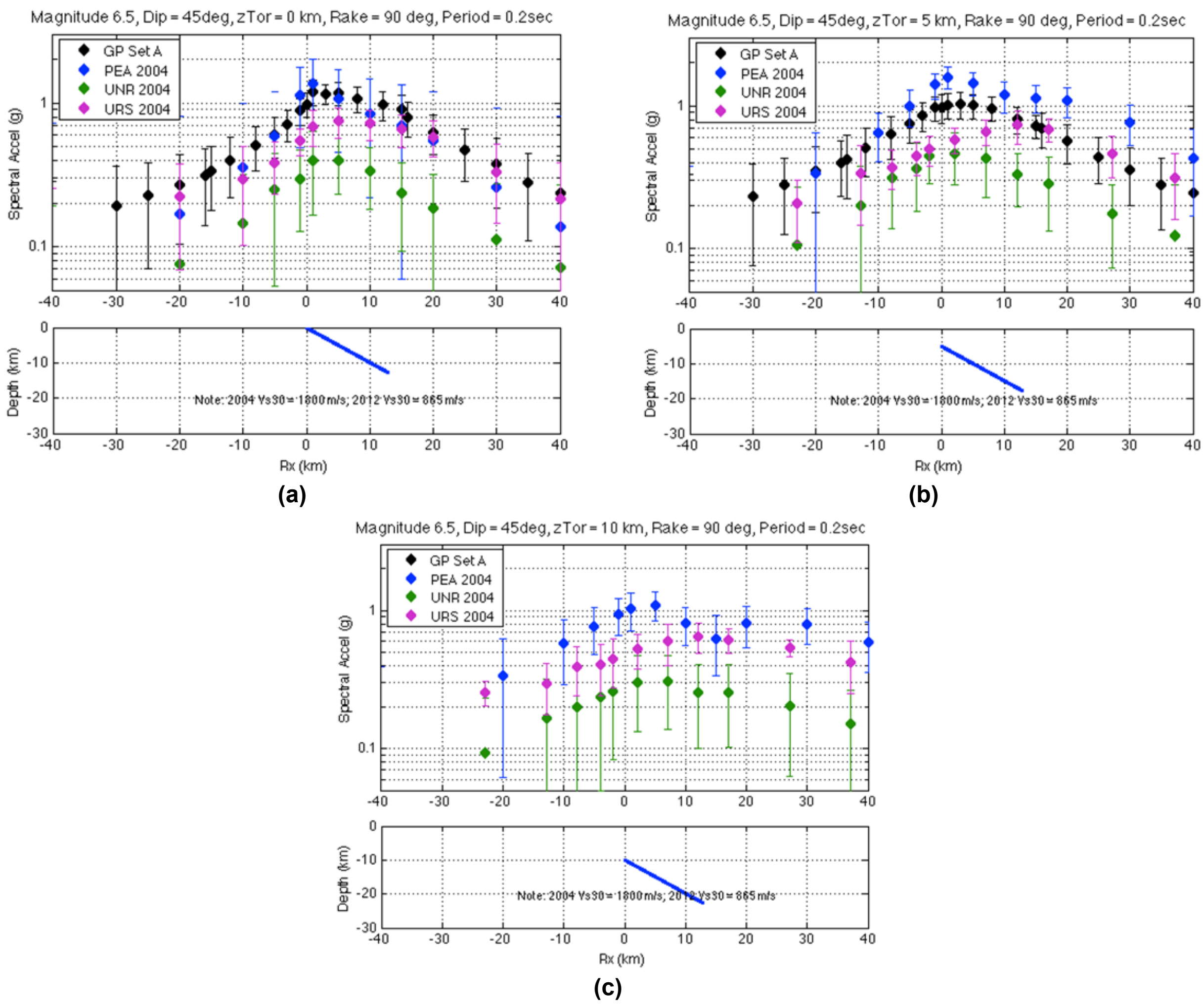

Figure 2.6 **Comparison of 2004 and 2012 models; shown here are M6.5 with a dip of 45º with varied depths: (a) 0 km, (b) 5 km, and (c) 10 km.**

3 The New Hanging-Wall Model

3.1 MODEL DEVELOPMENT

The new HW model was developed to be amendable to a GMPE, meaning that the model could be an additional term added to the base form of a GMPE. As stated in Section 1, there is a lack of available empirical data for which to constrain the HW scaling. Simulations add a level of understanding to the HW effect, but models used in 2004 were divergent in their results. The most recent sets of simulations have updated the 2004 models and now provide a more representative suite of possible ground motions. For this reason, the simulation results from GP Set A and Set B were used in the HW model development.

3.1.1 Footwall Functional Form

To develop the HW model, the first step is to build the functional form equation based on a regression of the simulation results for the FW side of the fault. Using this methodology, the equation for the functional form of the results from the GP model simulations was developed and is shown in Equation (3.1).

$$\ln\left(S_a\right) = b_1 + \left[b_2 + b_3 * \left(\mathbf{M} - 6\right)\right] * \left\{\ln\left[\left(R_{RUP}\right) + b_4\right]\right\} + b_5 * \left(\mathbf{M} - 6\right) + b_6 * \left(\mathbf{M} - 6\right)^2 + b_7 * \left(R_{RUP}\right) \tag{3.1}$$

where **M** is magnitude, R_{RUP} is distance measurement [(km)], and b_1–b_7 are coefficients of the functional form.

Additional event scaling terms were added to the functional form after significant dependence of the residuals on the dip of the fault and the depth to the top of the rupture were found. Additional terms for the dip of the fault and the depth to top of rupture (Z_{TOR}) were added to the functional form, for the FW regression GMPE, as shown in Equation (3.2).

$$\begin{aligned}\ln\left(S_a\right) = b_1 + \left[b_2 + b_3 * \left(\mathbf{M} - 6\right)\right] * \left\{\ln\left[\left(R_{RUP}\right) + b_4\right]\right\} + b_5 * \left(\mathbf{M} - 6\right) + b_6 * \left(\mathbf{M} - 6\right)^2 \\ + b_7 * \left(R_{RUP}\right) + f_{dip}\left(\delta\right) + f_{ZTORFW}\left(Z_{TOR}, \delta, \mathbf{M}\right)\end{aligned} \tag{3.2}$$

The dip and depth to top-of-rupture terms for the FW regression are given in Equations (3.3) and (3.4).

$$f_{dip}(\delta) = d_1 * (90 - \delta) + d_2 * (90 - \delta)^2 + d_3 \tag{3.3}$$

$$f_{ZTORFW}(Z_{TOR}, \delta, \mathbf{M}) = \left[z_{ft1} * (90 - \delta) + z_{ft2}\right] + \left[z_{ft3} * (\mathbf{M} - 6)\right] \tag{3.4}$$

where δ is the dip of the fault, Z_{TOR} is the depth to the top of the rupture (km), d_1–d_3 are the coefficients of the dip equations, and z_{ft1}-z_{ft3} are the coefficients of the depth to the top-of-rupture equations. Using Equation (3.2), the regression for the FW simulation results for **M**6–**M**7.5 is shown in Figure 3.1. This form provides for an unbiased model on the FW side of the fault. The coefficients for Equations (3.2), (3.3), and (3.4) are available in Appendix B.

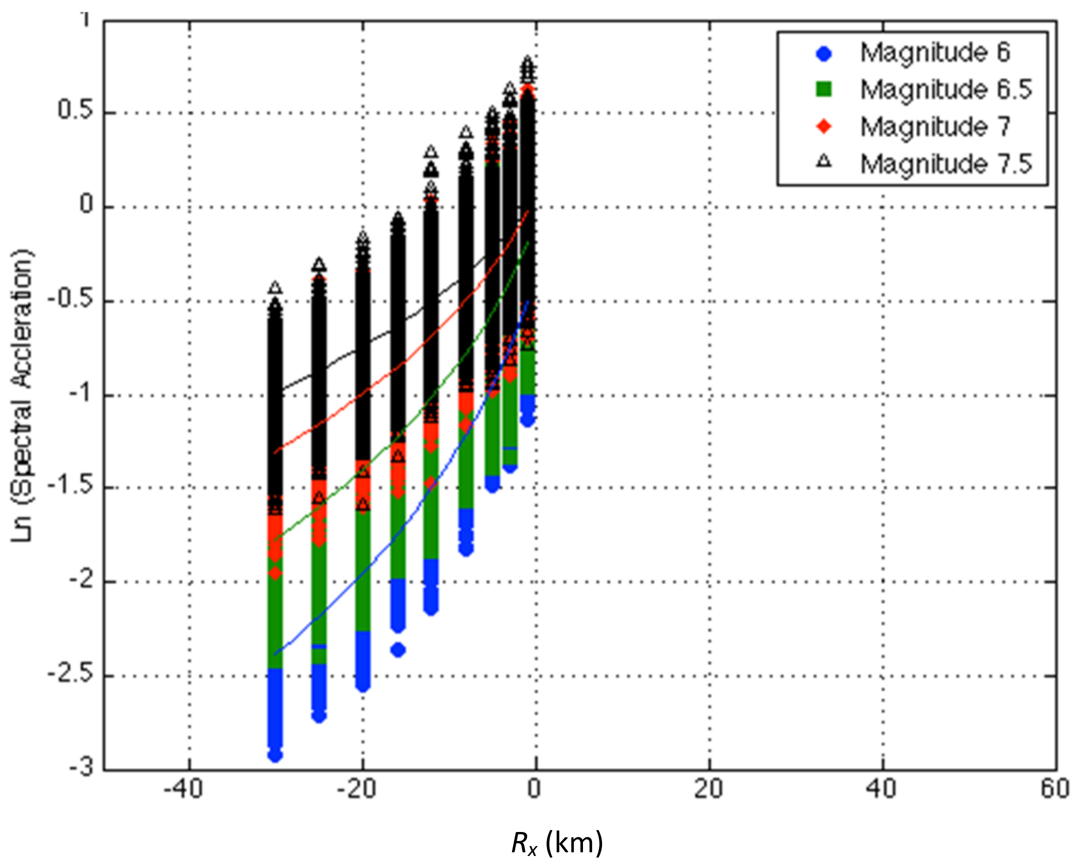

Figure 3.1 Regression of the median spectral acceleration (in natural log units) on the footwall for four magnitudes.

3.1.2 Hanging-Wall Terms

The next step to building the HW model is to compare the effect of the HW to the FW GMPE [Equation (3.2)]. The FW GMPE is shown as the dashed black line in Figure 3.2a. The mean spectral acceleration for each R_x was then computed, as shown by the red squares in Figure 3.2a. The residuals, which represent the overall HW effect, are shown in Figure 3.2b.

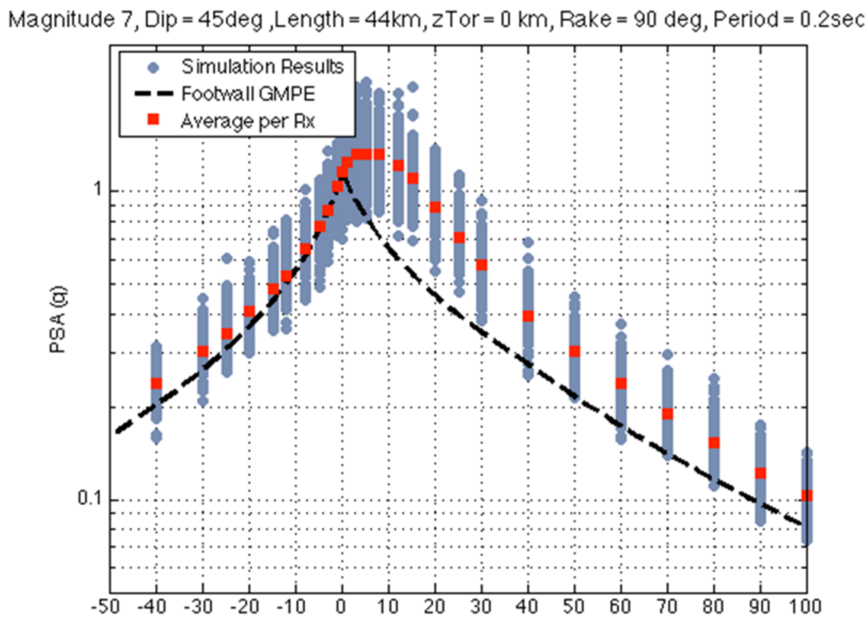

(a)

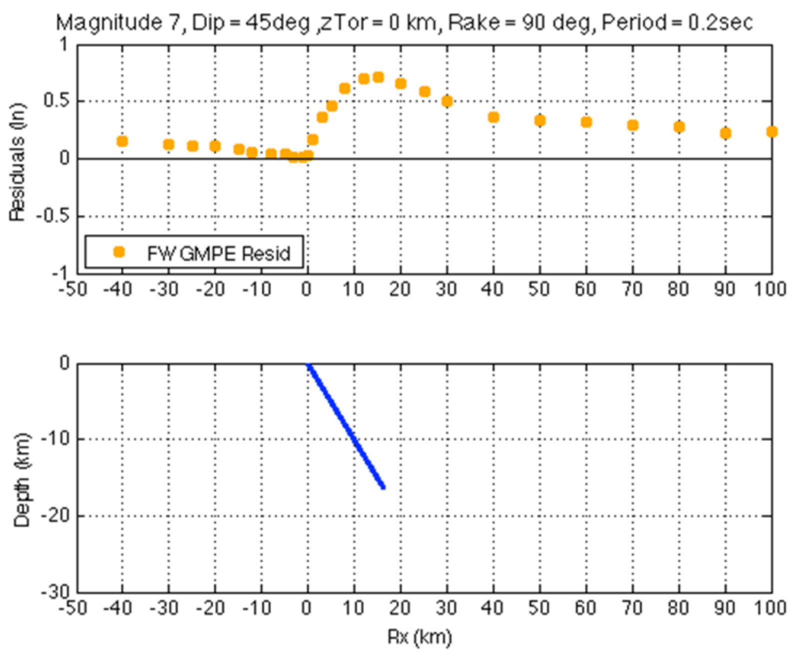

(b)

Figure 3.2 **(a) Application of the footwall GMPE (black dashed line) to the hanging-wall side of the fault. Red squares are representative of the mean acceleration (in *g*'s) for each R_x distance, and (b) residuals of mean acceleration to the footwall GMPE.**

Using the residuals of the unbiased model form of the median ground motion on the FW side of the fault [Equation (3.2)], the full HW model takes the form of Equation (3.5). This form of the HW effect model was developed so that it could be easily incorporated into the forms of the GMPEs being used in the NGA-West2 project.

$$\ln\left(S_a\right)=b_1+\left[b_2+b_3*\left(\mathbf{M}-6\right)\right]*\left\{\ln\left[\left(R_{RUP}\right)+b_4\right]\right\}+b_5*\left(\mathbf{M}-6\right)+b_6*\left(\mathbf{M}-6\right)^2+b_7*\left(R_{RUP}\right)$$
$$+f_{dip}\left(\delta\right)+f_{ZTORFW}\left(Z_{TOR},\delta,\mathbf{M}\right)+f_{hw}\left(\mathbf{M},\delta,W,Z_{\mathrm{TOR}},R_x,R_y,L\right) \tag{3.5}$$

The HW term is composed of an amplitude term (a_1) and five scaling terms: dip, magnitude, distance perpendicular to the rupture, Z_{TOR}, and distance off the end of the rupture. The model of the HW effect, f_{hw}, is given by:

$$f_{hw}\left(\mathbf{M},\delta,W,Z_{TOR},R_xR_yL\right)=a_1T_1\left(\delta\right)T_2\left(\mathbf{M}\right)T_3\left(R_x,W,\delta,\mathbf{M}\right)T_4\left(Z_{TOR}\right)T_5\left(R_x,R_y,L\right) \tag{3.6}$$

The amplitude term, a_1, is scaled for a **M**6.5 event, with a dip of 45º, and a surface rupture with a maximum effect at a distance equal to the surface projection of the bottom edge of the fault. The form of Equation (3.6) is flexible in that it allows the individual developers of the GMPEs to adopt the scaling from the simulations that they consider to be reliable, while still using the empirical data to constrain the amplitude, a_1, or other specific tapers in the model.

3.1.2.1 T_1 –Dip Scaling

The dip scaling term was designed to be centered for a fault with a 45º dip and takes the form as shown below.

$$T_1\left(\delta\right)=\left(90-\delta\right)/45 \qquad \text{for } \delta\le 90^\circ \tag{3.7}$$

This model is applicable for dips of 30°or more, but, as will be shown later, the simulated data are not consistent with this model for dips less than 30°. It is currently not clear as to the cause for the change in scaling for dips less than 30° from the simulated data.

3.1.2.2 T_2 – Magnitude Scaling

The magnitude scaling term was designed to be centered for a **M**6.5 event with and takes the form as shown below.

$$T_2\left(\mathbf{M}\right)=1+a_2\left(\mathbf{M}-6.5\right) \tag{3.8}$$

The smallest magnitude considered in the 34 scenarios is **M**6.0. The scaling from Equation (3.8) does not go to zero at **M**6; therefore, the extrapolation of the magnitude scaling below **M**6 is not constrained and must be set by the GMPE developers.

3.1.2.3 T_3 – Distance Scaling

The distance scaling term is dependent on the distance away from the fault. If the station location has a negative R_x value, it is assumed to be on the FW and is therefore zero. When the location is on the HW side of the fault, three distance metrics are used to describe the distance dependence. Directly over the HW, the distance function increases parabolically with increasing distance from the fault [f_1 term, Equation (3.11)]. Using the f_1 equation, the HW effect reaches it maximum value over the bottom edge of the rupture. As the distance increases further from the fault, the f_2 term [Equation (3.12)] is utilized until R_x is greater than the R_2 term [Equation (3.10)]. Using the f_2 term, the HW effect decreases parabolically with distance from the surface projection of the bottom edge of the fault. At greater distances than R_2, the HW effect decreases exponentially using the f_3 term [Equation (3.13)]. The shape of the distance taper is shown in the Figure 3.3.

$$T_3\left(R_x, W, \delta, \mathbf{M}\right) = \begin{cases} 0 & \text{for } R_x < 0 \\ f_1 & \text{for } R_x \le R_1 \\ f_2 & \text{for } R_x > R_1 \text{ and } R_x \le R_2 \\ f_3 & \text{for } R_x \le R_2 \end{cases}$$

$$R_1\left(W, \delta\right) = W * \cos\left(\delta\right) \tag{3.9}$$

$$R_2\left(\mathbf{M}\right) = 62 * \left(\mathbf{M}\right) - 350 \tag{3.10}$$

$$f_1\left(R_x\right) = h_1 + h_2\left(R_x/R_1\right) + h_3\left(R_x/R_1\right)^2 \tag{3.11}$$

$$f_2\left(R_x\right) = h_4 + h_5\left[\left(R_x - R_1\right)/\left(R_2 - R_1\right)\right] + h_6\left[\left(R_x - R_1\right)/\left(R_2 - R_1\right)\right]^2 \tag{3.12}$$

$$f_3\left(R_x, \mathbf{M}\right) = \left(h_4 + h_5 + h_6\right) * e^{\left[-\left(R_x - R_2\right) * \gamma\right]} \tag{3.13}$$

where $\gamma = -0.2\left(\mathbf{M}\right) + 1.65$, W is the width of the fault (km), and h_1–h_6 are the coefficients of the distance taper.

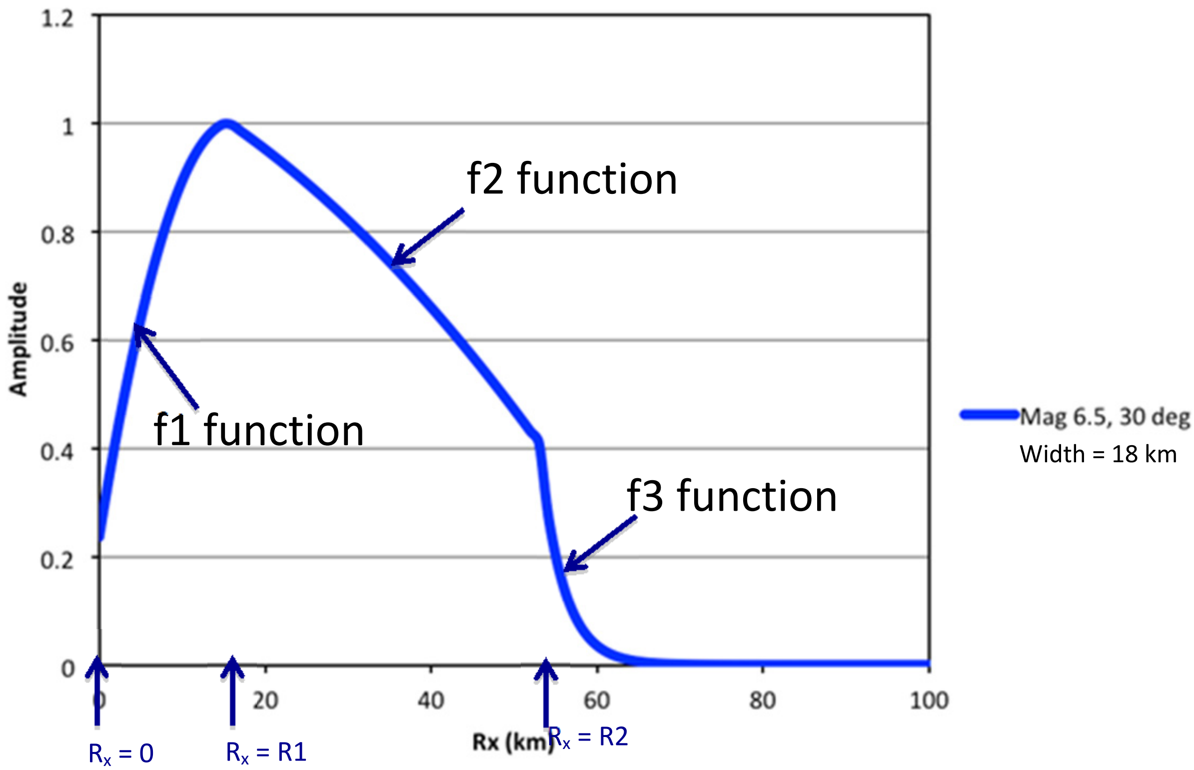

Figure 3.3 The distance taper, T_3, shown graphically

3.1.2.4 T_4 – Depth Scaling

Only two depths were modeled in the GP Set A and Set B simulation series: 0 km depth and 5 km depth. Because the amplitude of the HW effect for Z_{TOR} = 5 km is 30% smaller than the HW effect for surface rupture, there is a dependence on Z_{TOR}. However, with only two points, the form of the Z_{TOR} scaling is not constrained: it is not known if the scaling is linear between 0 and 5 km, nor is it known how the Z_{TOR} scaling extrapolates to Z_{TOR} values greater than 5 km.

3.1.2.5 T_5 – Rupture Edge Distance Scaling

The second distance scaling is a taper that is applied to sites located off the end of the rupture at source to site angles of 45–90º and from 90–135º. This taper allows for a gradual decrease in the HW effect at sites that are not within the length of the rupture (source-to-site angle of 90º). This taper is parameterized by an additional distance metric, R_y. If R_y is greater than half the rupture length (L/2), then the site is located off the end of the rupture. Therefore, the T_5 term is set to unity for sites located along the rupture with $R_y \leq L/2$.

$$T_5\left(R_x, R_y, L\right) = \begin{cases} 1 & \text{for } abs\left(R_x\right) \le L/2 \\ \left\{\left(0.577 * R_x + 5\right) - \left[abs\left(R_y\right) - L/2\right]\right\} / \left(0.577 * R_x + 5\right) & \text{for } L/2 < abs\left(R_y\right) < 0.577 * R_x + 5 + L/2 \\ 0 & \text{for } abs\left(R_y\right) \ge 0.577 * R_x + 5 + L/2 \end{cases} \tag{3.14}$$

where L is the length of the fault, (km), and $abs(R_y)$ is the distance dimension measured along the strike of the fault (km) [Ancheta et al. 2013].

Applying the functional form, site effects terms, and HW term as shown in Equation (3.5), the model is calculated for all distances along the FW and HW. An example of the final form is shown in Figure 3.6a and 3.6b. See Appendix B for the coefficients to the functional form, event terms and HW terms. See Appendix C for the result of the HW model applied to all GP model scenarios for periods 0.1, 0.2, 0.5, and 1.0 sec.

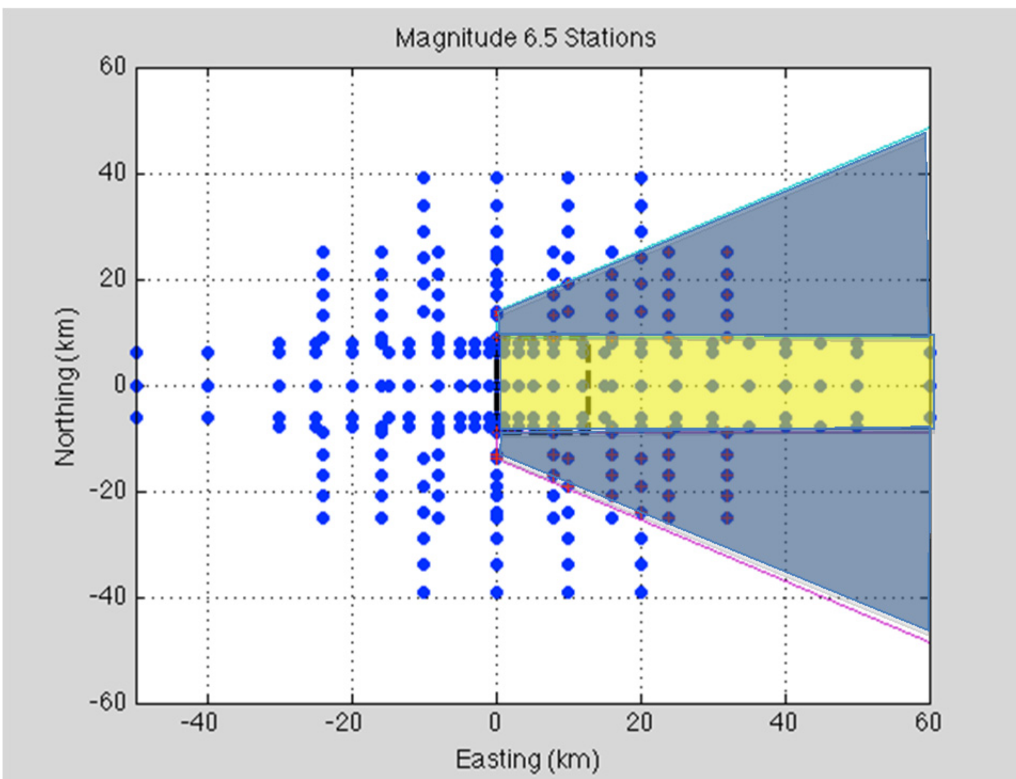

Figure 3.4 Example of the side taper for a M6.5 event. The side taper applies to stations located in the blue shaded areas.

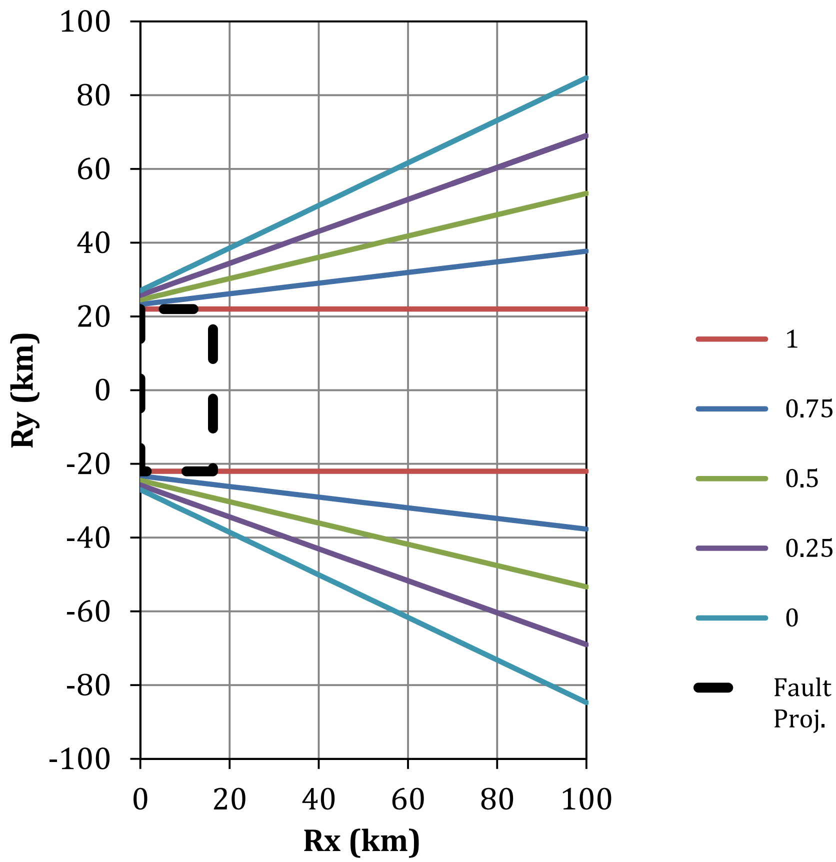

Figure 3.5 **Figure contour of a plot of the T_5 term. Example given is a M7 surface rupture, a length of 44 km, a width of 23 km, and with a dip of 45°.**

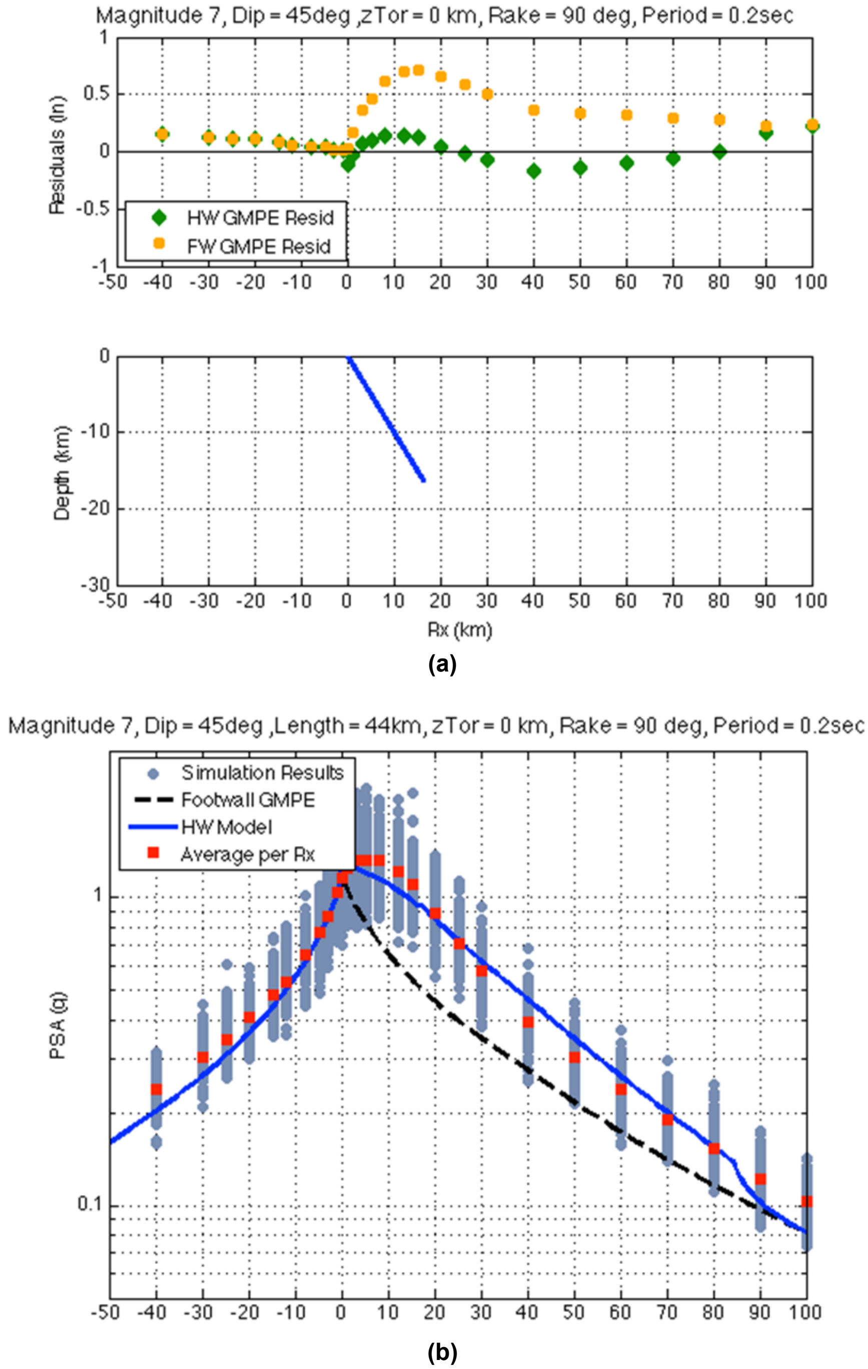

Figure 3.6 **(a) Application of the hanging-wall model (blue solid line to all stations along the fault; and (b) residuals from the footwall and hanging-wall model.**

3.1.3 Residuals for Hanging-Wall Model

The mean residuals by scenario are shown as a function of R_x in Figure 3.7 and Figure 3.8. In each case, the residuals are averaged over all sites with the same R_x values. The residuals for sites on the HW side of the rupture typically fall within the range -0.2 to 0.2 natural log units. The exception to this is small magnitude events with shallow dipping faults; for instance, the **M**6 and **M**6.5 with shallow dips of 20° and 30° and **M**7 with a shallow dip of 20°. It is still being investigated if the 2010 Graves and Pitarka one-dimensional velocity model within the top 7 km may be a cause of this or if this phenomenon may be a new issue to resolve. Near the surface trace of the top of the rupture (-1 km < R_x < 1 km), the model tends to overpredict the ground motions for **M**7.0–**M**7.5; however, this over-prediction at the top of the rupture is not seen for **M** 6–6.5 or for **M**7.8. For the **M**7.8 scenarios, the model overpredicts the HW effect at R_x distances greater than 10 km. Finally, the buried rupture residuals are well constrained, except as noted for the **M**6.5 with a shallow dip of 20°.

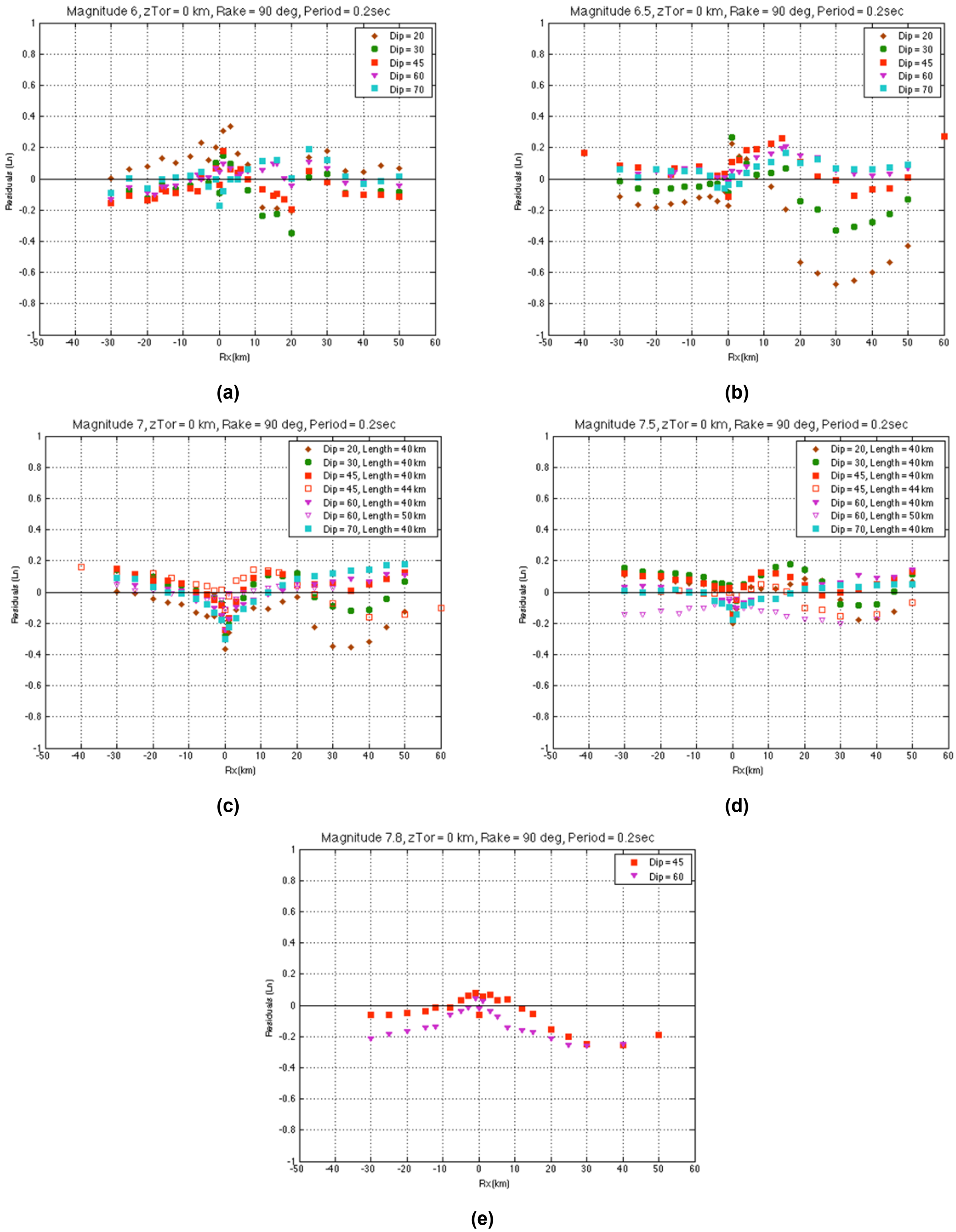

Figure 3.7 **Residuals (in natural log units) for surface ruptures. (a) M6, (b) M6.5, (c) M7, (d) M7.5, and (e) M7.8.**

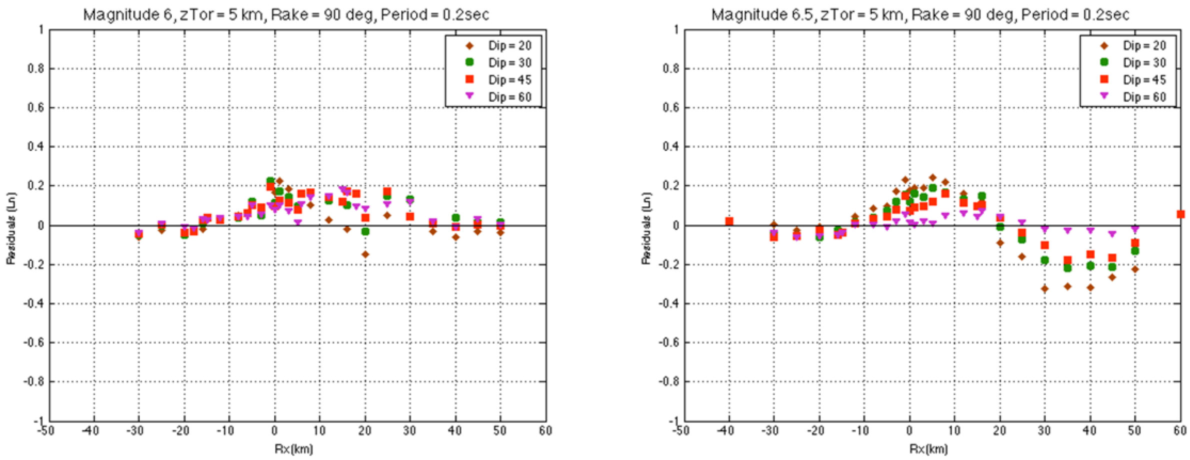

(a) **(b)**

Figure 3.8 Residuals (in natural log units) for buried ruptures (Z_{TOR} =5 km): (a) M6, and (b) M6.5.

3.2 COMPARISON OF MODEL TO 2004 SIMULATION RESULTS

The HW model is then compared to the results of the 2004 simulations. Because the HW model was developed from the GP models, the result of GP Set A and Set B simulations are not shown separately.

As shown in Figure 3.9, the HW model closely resembles the PEA and URS models for a **M**7 event with a dip of 45°. Note that as shown in Figure 1.2b, the 2008 NGA models also closely resemble each other for this event because of the availability of empirical data.

Like the 2004 URS model, the effect from the HW model increases in amplitude over the fault and decreases beyond a distance equals to the surface trace of the bottom of the fault, as shown in Figure 3.10. Interestingly, as the magnitude increases, the HW model more closely resembles the results from 2004 PEA.

The HW model for a buried rupture fits below the 2004 PEA model and above the 2004 UNR model, as shown in Figure 3.11. The HW model closely follows the 2004 URS model but only beyond the fault plane. At closer distances, the HW model's shape is more similar to that of the PEA and UNR models.

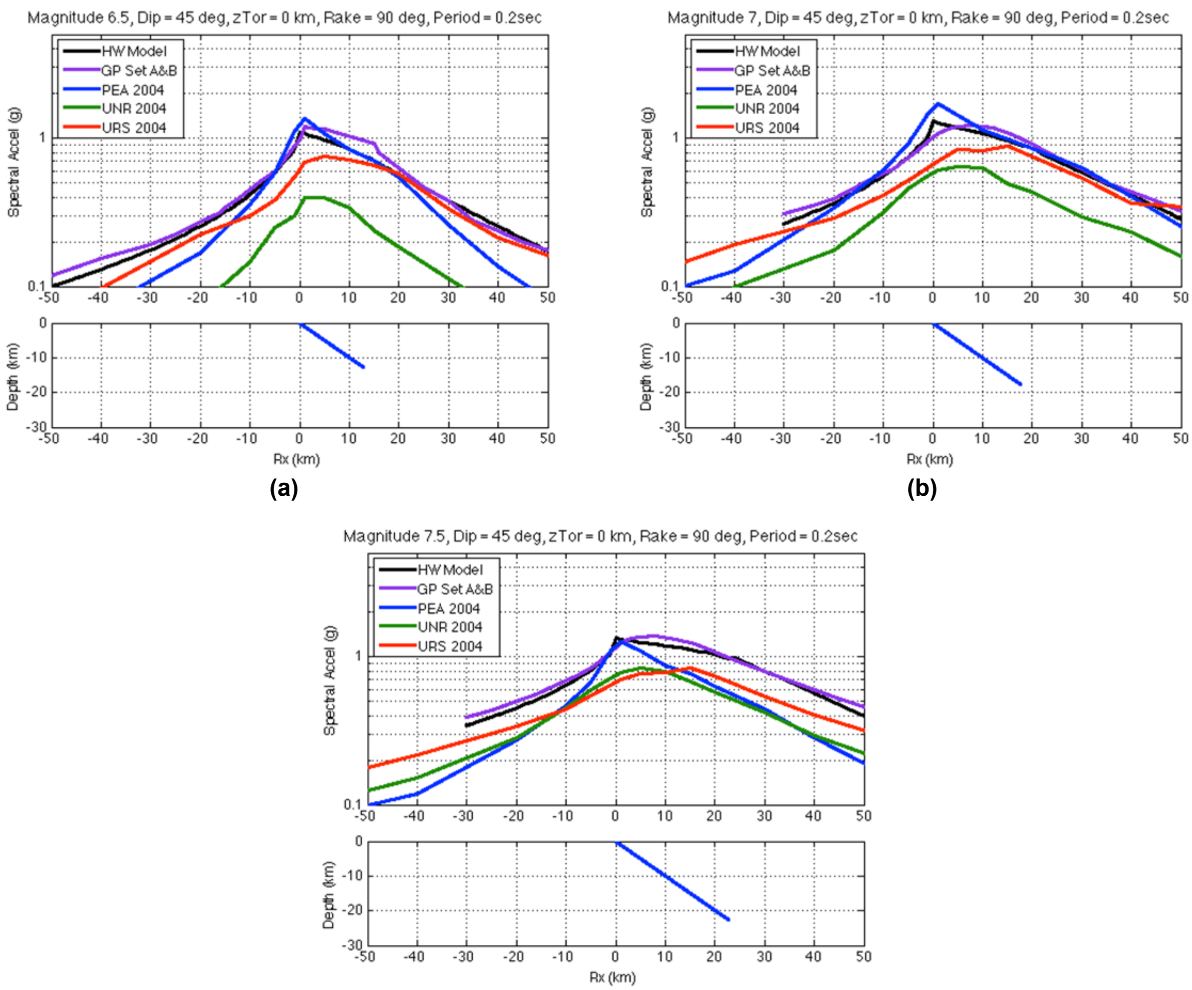

(c)

Figure 3.9 Comparison of the median acceleration (in *g*'s) for 2004 models and hanging-wall model; shown here are surface ruptures with a dip of 45º with varied magnitudes: (a) M6.5, (b) M7, and (c) M7.5.

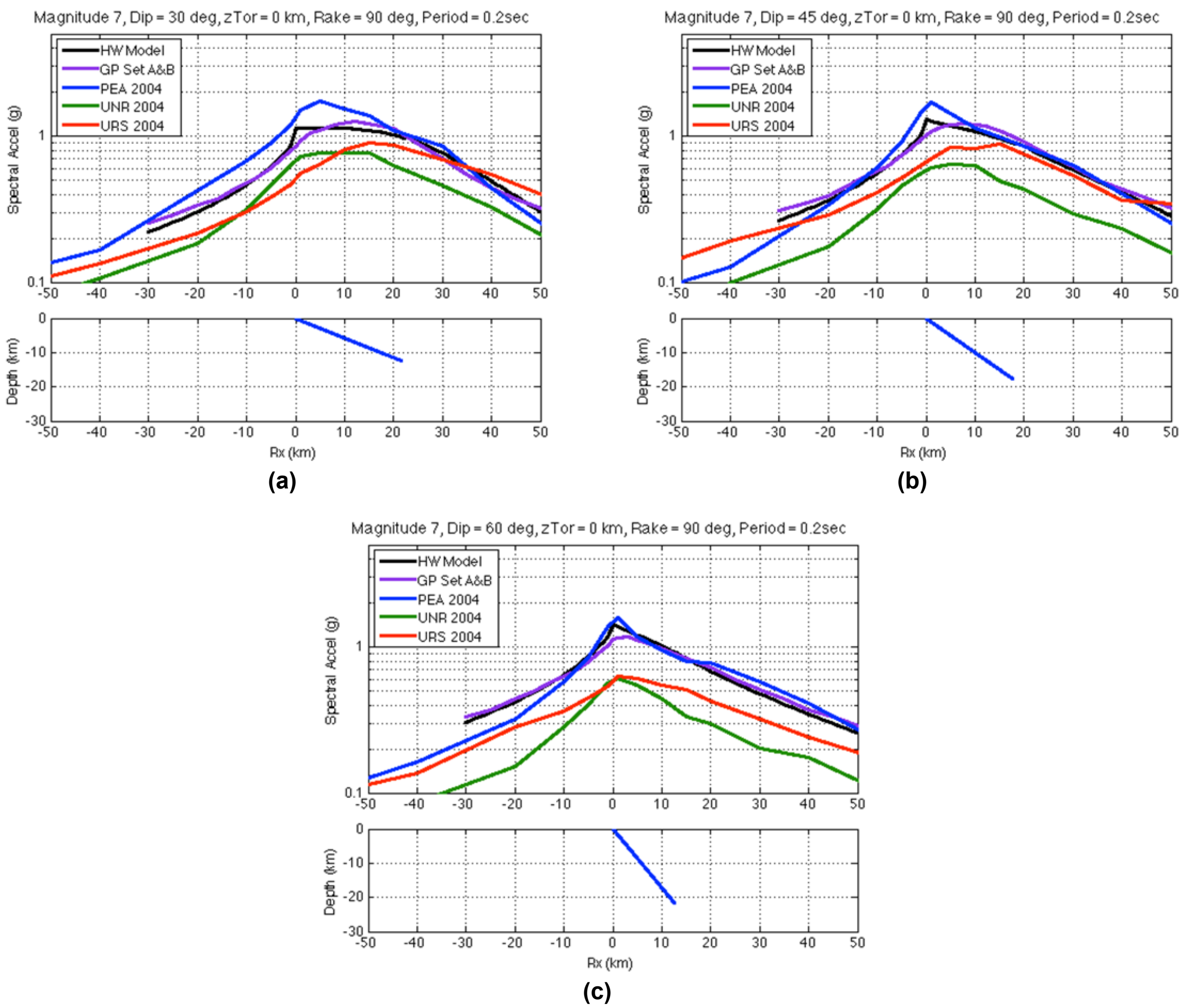

Figure 3.10 **Comparison of the median acceleration (in *g*'s) for 2004 models and hanging-wall model; shown here are M7 surface ruptures with varied dips: (a) 30º, (b) 45º, and (c) 60º.**

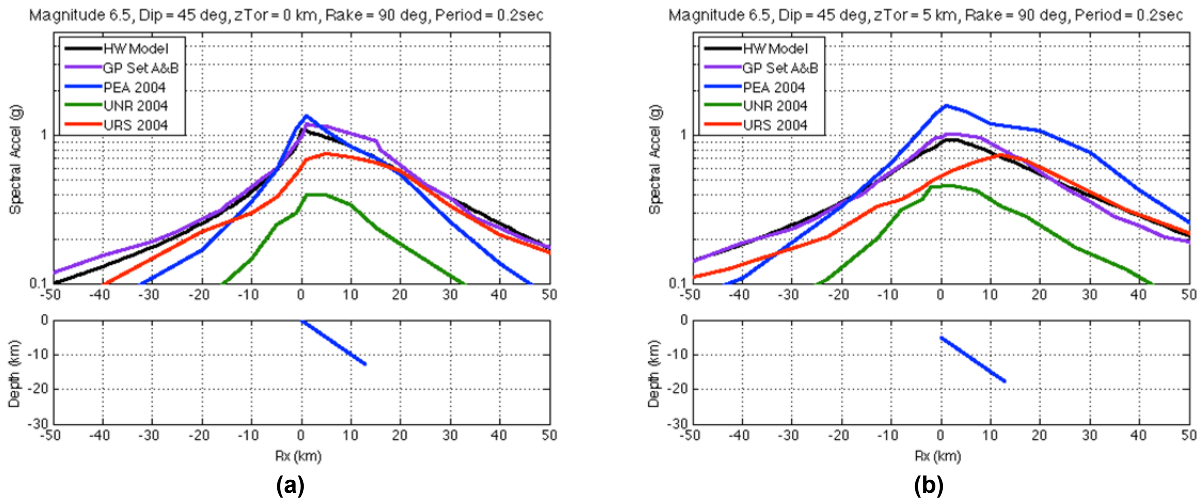

Figure 3.11 **Comparison of the median acceleration (in *g*'s) for 2004 models and hanging-wall model; shown here is a M6.5 event with a dip of 45º with varied depths: (a) 0 km, and (b) 5 km.**

3.3 COMPARISON BETWEEN MODEL AND NGA (2008)

As stated in Section 1, more empirical data was available when developing the 2008 NGA models. In the Appendix D figures, the HW model is compared to the spectral shapes of the five 2008 NGA models with respect to magnitude scaling (Appendix D-1 through Appendix D-4), dip of the fault (Appendix D-5 through Appendix D-7), and depth to the top of rupture (Appendix D-8).

The HW model closely resembles the 2008 NGA models for the small magnitude events, as seen in Appendix D-1. As the magnitude increases, however, the remaining the 2008 NGA relationships attenuate much quicker with distance from the fault. As seen in Appendix D-4, at an R_x distance of 30 km, the spectral acceleration is approximately 0.5 natural log units great than the 5 GMPEs. Whether this is an artifact of the lack of empirical data at this distance or an issue with attenuation of the GP model is yet to be resolved.

Just as there is a discrepancy between the five 2008 NGA models at shallow dip angles, so is there a discrepancy between the HW model and the other 5 GMPEs, as shown in Appendix D-5. The 2008 Abrahamson and Silva, 2008 Chiou and Youngs and 2008 Campbell and Bozorgnia models all represent the HW as having the greatest effect near the top of the fault, then decreasing over the fault, with an exponential decrease beyond the fault. As stated in Section 3.1.2.3, using the GP model results to develop the HW distance taper, the HW effect increases over the fault, which is in opposition to the previously three mentioned 2008 NGA models. Again, the HW model does not attenuate with distance as quickly as the 2008 NGA models.

For buried ruptures, the spectral shape of the HW effect is different from the 2008 NGA models as seen in Appendix D-8. Except for the 2008 Idriss model, the HW effect is less than the other four GMPEs at close distances (e.g., less than 15 km), yet greater than all GMPEs at greater distances.

3.4 COMPARISON BETWEEN MODEL AND EMPIRICAL DATA FROM NGA-WEST2 DATABASE

Using the 15 events listed in Section 1.3, the intra-event residuals for the 2008 Abrahamson and Silva and the 2008 Chiou and Youngs models, utilizing the HW term, were compared to the HW term. Figure 3.12 shows selected comparisons; all events from Table 1.1 can be viewed in Appendix E. As seen in Figure 3.12, the HW term correlates well for the Imperial Valley, Northridge, and Wenchuan events; however, for the Chi-Chi and L'Aquila events the HW term is lower than the observed recording.

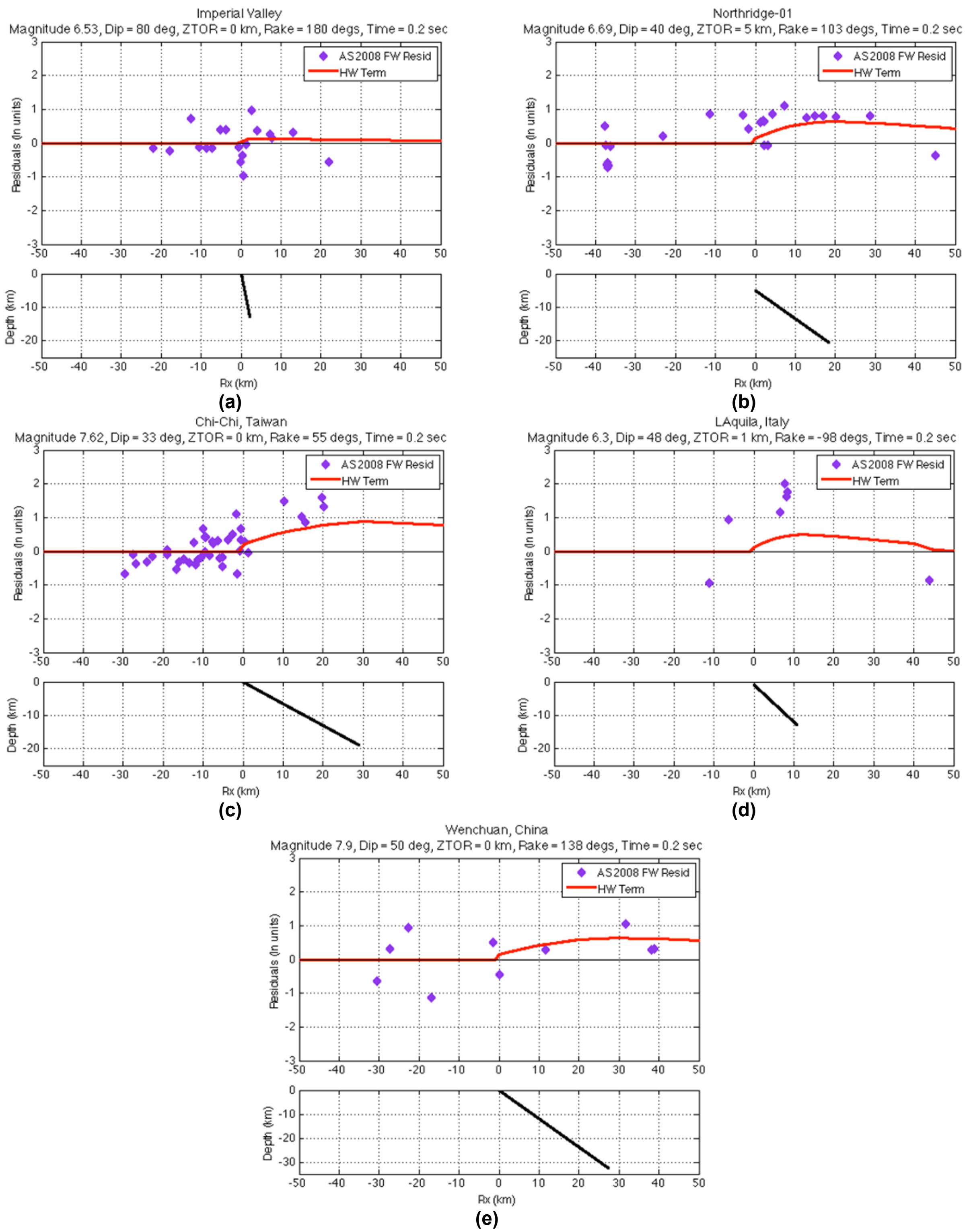

Figure 3.12 **Intra-event Residuals (in natural log units) for selected events with at least five recordings within 80 km, and at least one recording on the footwall with R_{JB} distances of 15 km or less, and three or more recordings directly over the rupture plane: (a) Imperial Valley, (b) Northridge, (c) Chi-Chi, (d) L'Aquila, and (e) Wenchuan.**

3.5 COMPARISON BETWEEN MODEL AND NGA-W2 MODELS

The NGA-West2 project was undertaken by PEER to expand the previous work described in Section 1.2 of this report. This work culminated in the NGA-West2 GMPEs derived from the expanded NGA-West2 database described in Section 1.3.

The Abrahamson, Silva, and Kamai (ASK13) [2013] and the Campbell and Bozorgnia (CB13) [2013] GMPEs used parts of the simulation-based HW model to constrain the HW scaling in their GMPEs for sites located over the surface projection of the rupture plane. The Chiou and Youngs (CY13) [2013] GMPE does not use the HW model described within this paper, but instead relies on a HW term that better fits with their base functional form. The Boore, Stewart, Seyhan and Atkinson (BSSA13) [2013] GMPE does not specifically include a HW term, but the effect of the HW is implicitly captured by the use of the R_{JB} distance term. The Idriss (I2013) [2013] GMPE does not include a HW term, nor does it attempt to capture differences between the ground motion on the FW and HW.

Figures 3.13 through 3.15 compares the HW scaling from the five models to the HW scaling from the simulations. In each figure, the ground motion is normalized to the FW motion at an R_x distance of 12 km to remove differences in the GMPEs on the FW from the HW predictions. Figure 3.13 compares the GMPEs for a range of magnitudes for a fixed dip of 45°. Figure 3.14 compares the HW scaling for different dip angles for **M**7 earthquakes; Figure 3.15 compares the HW scaling for different Z_{TOR} values. These comparisons show that for sites located over the rupture plane, the GMPEs with HW effects tend to have larger HW factors than the HW model from the simulations;however, the HW scaling simulations are similar to the R_{JB}-based BSSA model. At large distances (R_x > 20 km), the simulations show a much weaker attenuation than all of the GMPEs.

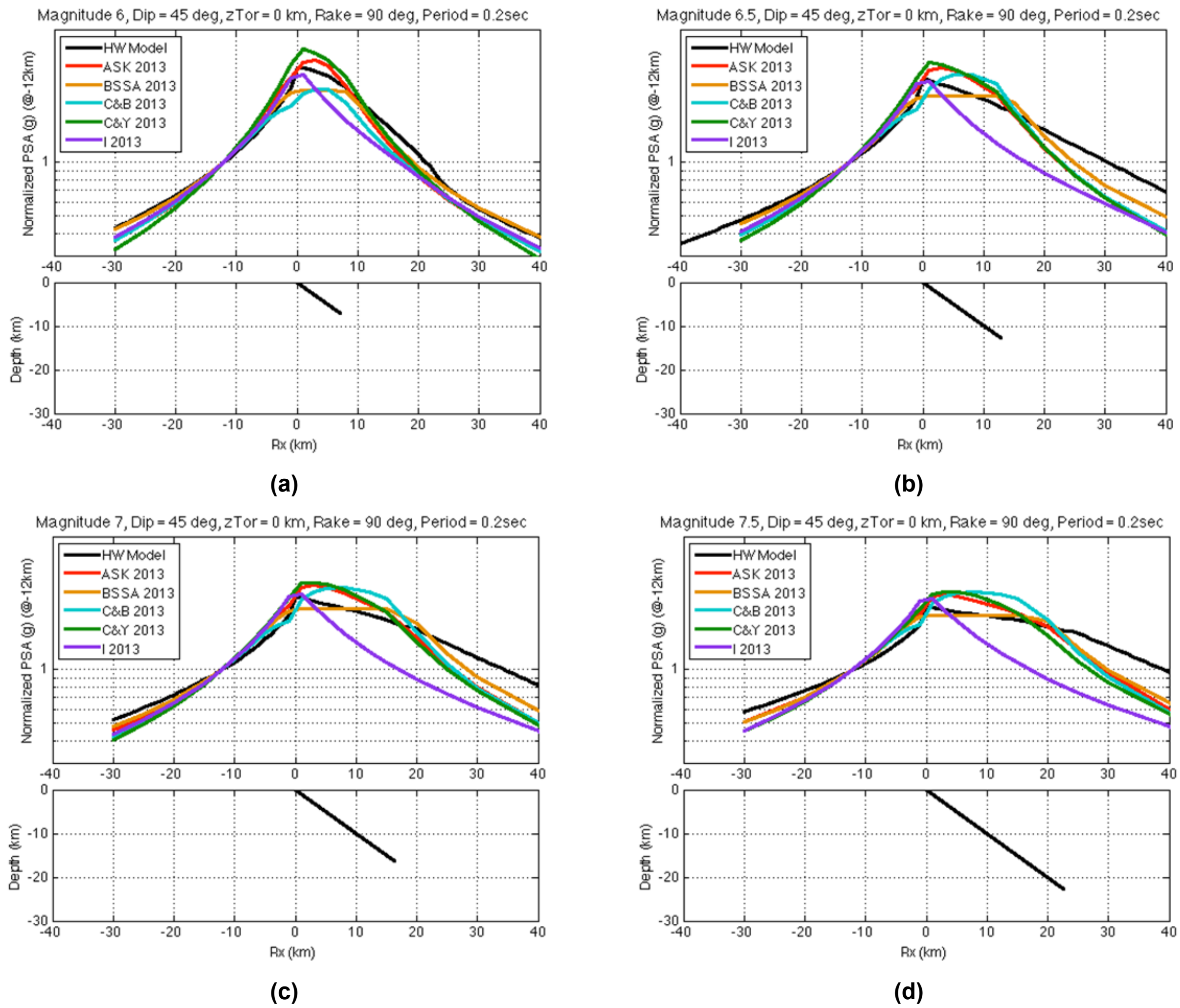

Figure 3.13 **Comparison of the hanging-wall results for five 2013 NGA-West2 models; shown here are surface ruptures with a dip of 45º with varied magnitudes: (a) M6, (b) M6.5, (c) M7, and (d) M7.5.**

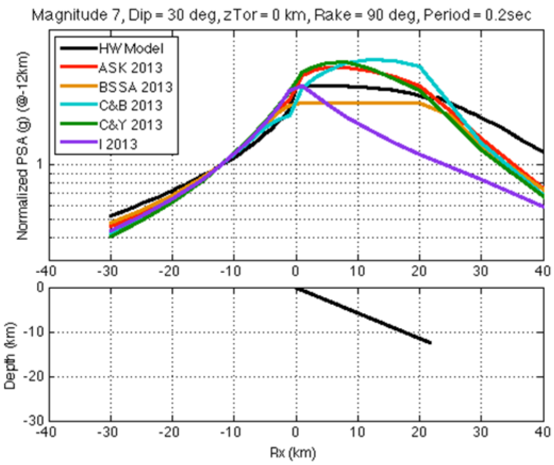

(a)

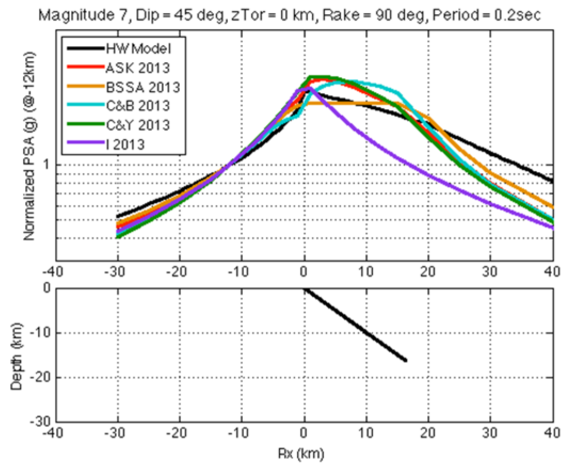

(b)

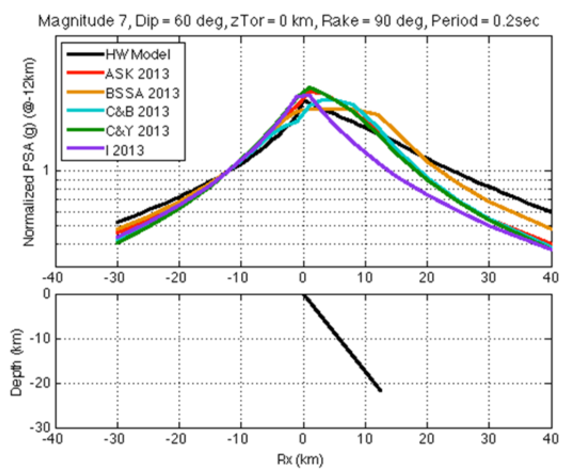

(c)

Figure 3.14 Comparison of the median acceleration (in *g*'s) for the 2013 models and hanging-wall model. Models have been normalized at an R_x = -12 km; shown here are M7 surface ruptures with varied dips: (a) 30°, (b) 45°, and (c) 60°.

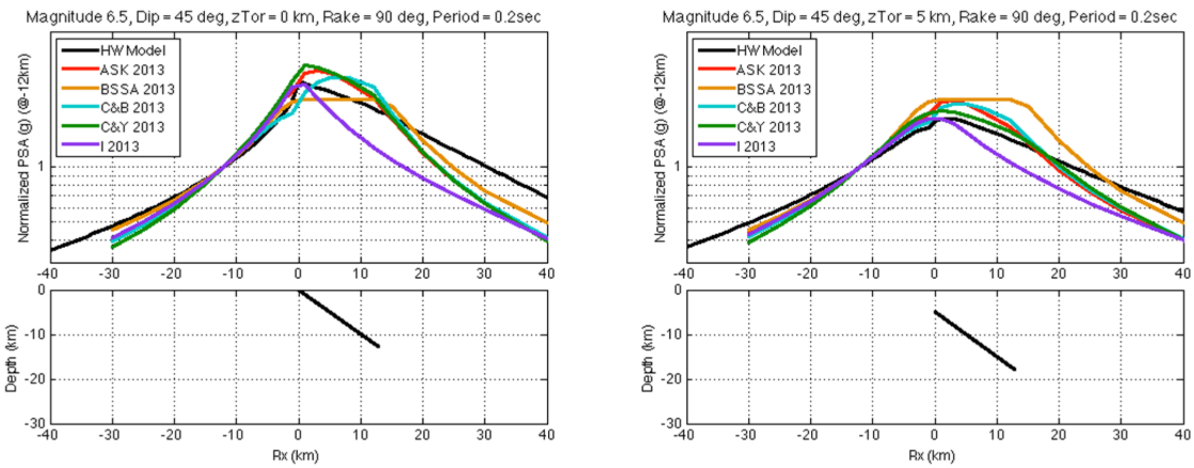

(a) (b)

Figure 3.15 **Comparison of the median acceleration (in *g*'s) for the 2013 models and hanging-wall model. Models have been normalized at an R_x = -12 km; shown here are M6.5 events with a dip of 45º with varied depths: (a) 0 km, and (b) 5 km.**

4 Vertical Hanging-Wall Results

Rather than deriving a new model for the scaling of the HW for the vertical component, we provide comparisons of the scaling between the horizontal and vertical components from the simulated ground motions. This allows the GMPE developers to evaluate the need for a change in the scaling of the HW effects between the horizontal and vertical. This approach to the vertical HW effect is also better suited for models that use the V/H ratio approach for the vertical component.

We show examples of the comparison of the HW effects for the horizontal and vertical components for three cases. Figure 4.1 shows the HW scaling for a dip of 45° for **M**6, 6.5, 7.0, 7.5, and 7.8. For this case, the HW effects for the vertical component are similar to the HW effects on the horizontal component. Figure 4.2 shows the HW scaling for **M**7 earthquakes for dips ranging from 20–70°. For this case, the HW effects for the vertical and horizontal component are similar for dips of 45 and 60°, but there are differences over the rupture for shallow dips (20–30°) and steep dips (70°). Finally, Figure 4.3 shows the HW scaling for **M**6.5 earthquakes with a dip of 45° for depth to top of ruptures of 0 and 5 km. For this case, the HW effects for the vertical and horizontal component are similar. The full set of comparisons for all of the cases are shown in Appendix F.

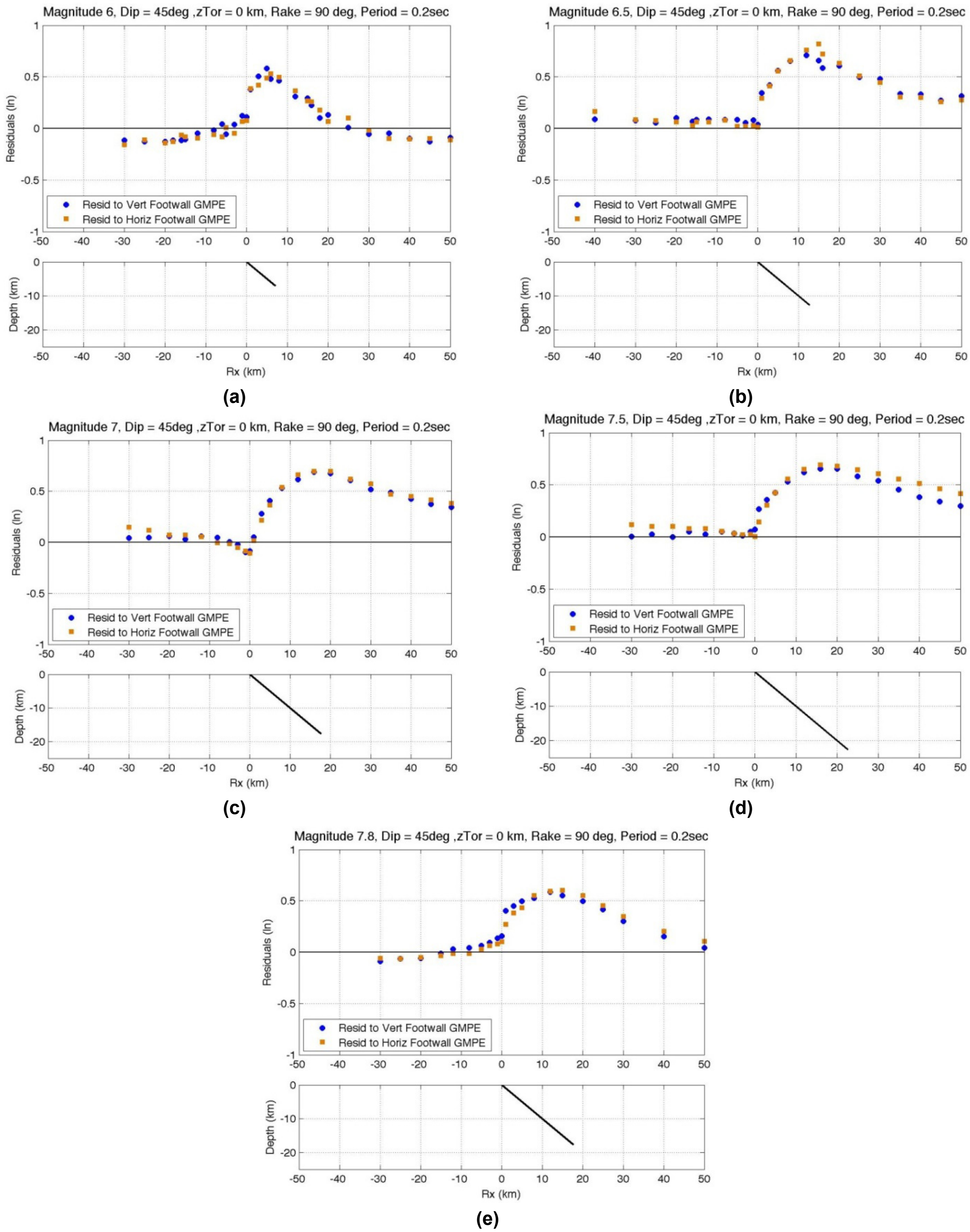

Figure 4.1 Comparison of the residuals (in natural log units) for the vertical footwall GMPE compared to the horizontal hanging-wall term; shown here are surface ruptures with a dip of 45º with varied magnitudes: (a) M6.0, (b) M6.5, (c) M7, (d) M7.5, and (e) M7.8.

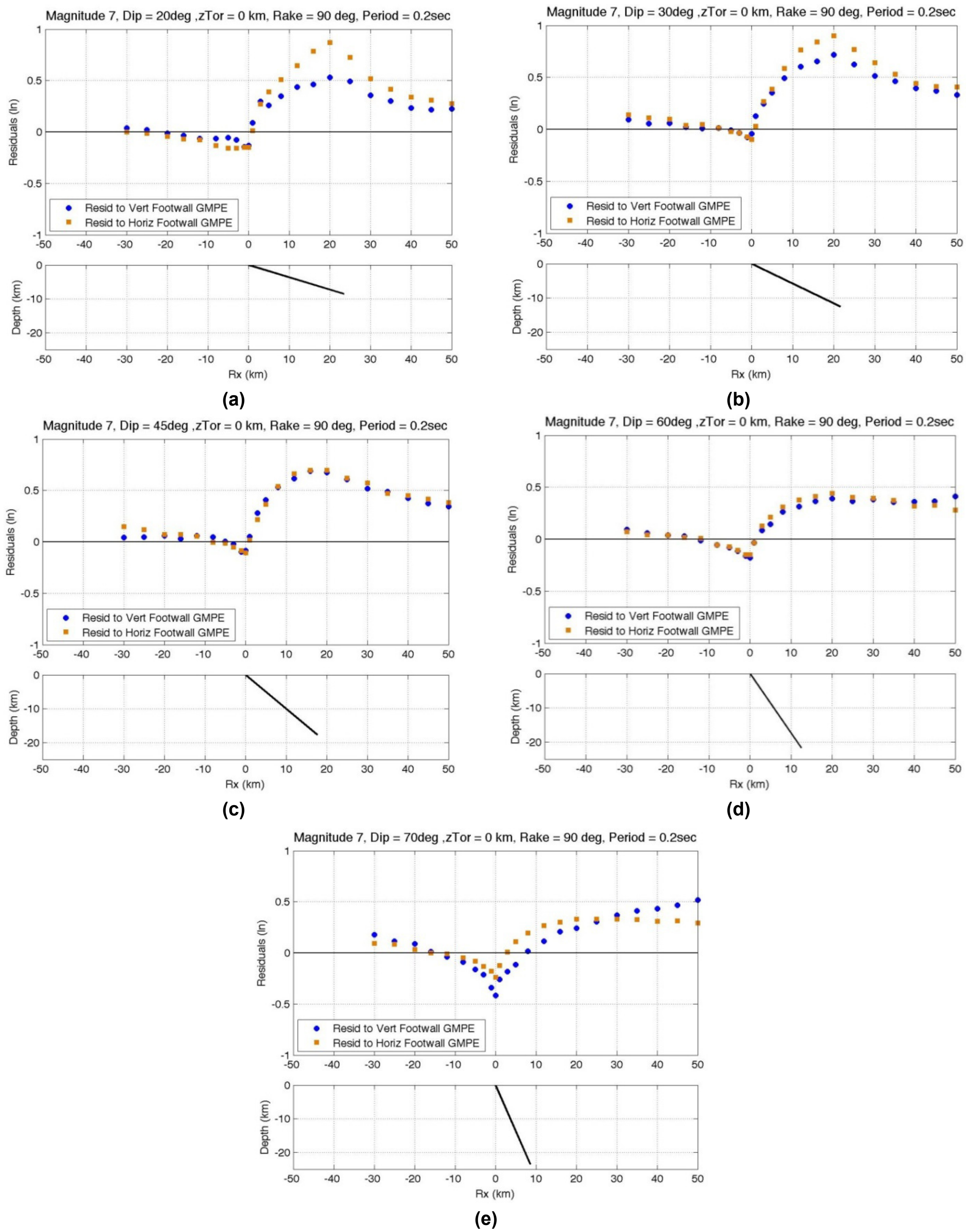

Figure 4.2 **Comparison of the residuals (in natural log units) for the vertical footwall GMPE compared to the horizontal hanging-wall term; shown here are M7 surface ruptures with varied dips: (a) 20º, (b) 30º (c) 45º, (d) 60º, and (e) 70°.**

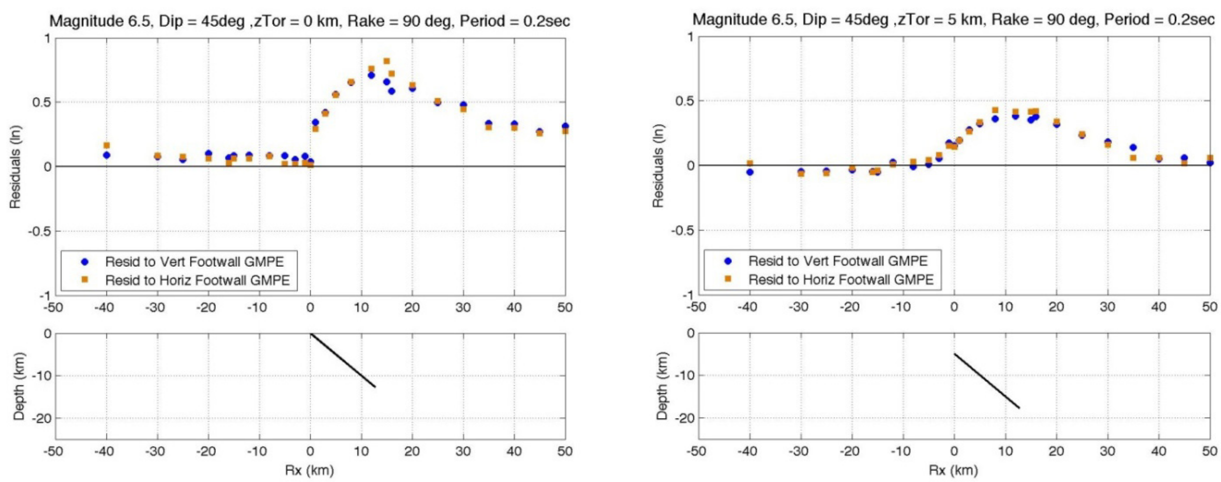

(a) **(b)**

Figure 4.3 **Comparison of the residuals (in natural log units) for the vertical footwall GMPE compared to the horizontal hanging-wall term; shown here are M6.5 events with a dip of 45º with varied depths: (a) 0 km and (b) 5 km**

REFERENCES

Abrahamson N.A., Somerville P.G. (1996). Effects of the hanging-wall and footwall on ground motions recorded during the Northridge earthquake, *Bull. Seismol. Soc. Am.,* 86(1B): S93-S99.

Abrahamson, N.A. and Silva, W. (2008), Summary of the Abrahamson and Silva NGA ground Motion Relations, *Earthq. Spectra*, 24(1): 67–97.

Abrahamson N.A., Atkinson G.M., Boore D.M., Bozorgnia Y., Shantz T., Roblee C. (2008): Comparisons of the NGA ground-motion relations, *Earthq. Spectra*, 24(1): 45–66.

Abrahamson N.A., Silva W.J., Kamai R. (2013). Update of the AS08 ground-motion prediction equations based on the NGA-West2 data set, *Report PEER 2013/04*, Pacific Earthquake Engineering Research Center, University of California, Berkeley, CA.

Ancheta T.D., Darragh R.B., Stewart J.P., Seyhan E., Silva W.J., Chiou B.S-J., Wooddell K.E., Graves R.W., Kottke A.R., Boore D.M., Tadahiro K., Donahue J.L. (2013) PEER NGA-West2 database, *Report PEER 2013/03*, Pacific Earthquake Engineering Research Center, University of California, Berkeley, CA.

Boore D.M, Atkinson G.M. (2008), Ground-motion prediction equations for the average horizontal component of PGA, PGV, and 5%-damped PSA at spectral periods between 0.01 s and 10.0 s, *Earthq. Spectra*, 24(1): 99–138.

Boore D.M., Stewart J.P., Seyhan E., Atkinson G.M. (2013). NGA-West2 equations for predicting response spectral accelerations for shallow crustal earthquakes. *Report PEER 2013/05*, Pacific Earthquake Engineering Research Center, University of California, Berkeley, CA.

Campbell K.W., Bozorgnia, Y. (2008). NGA ground motion model for the geometric mean horizontal component of PGA, PGV, PGD, and 5% damped linear elastic response spectra for periods ranging from 0.01 to 10 s, *Earthq. Spectra*, 24(1): 139–171.

Campbell K.W., Bozorgnia Y. (2013). NGA-West2 Campbell-Bozorgnia ground motion model for the horizontal components of PGA, PGV, and 5%-damped elastic pseudo-acceleration response spectra for periods ranging from 0.01 to 10 sec. *Report PEER 2013/06*, Pacific Earthquake Engineering Research Center, University of California, Berkeley, CA.

Chiou B.S-J., Youngs R. (2008), An NGA model for the average horizontal component of peak ground motion and response spectra, *Earthq. Spectra*, 24(1): 173–215.

Chiou B.S-J., Youngs R (2013). Update of the Chiou and Youngs NGA ground motion model for average horizontal component of peak ground motion and response spectra. *Report PEER 2013/0*7 Pacific Earthquake Engineering Research Center, University of California, Berkeley, CA.

Graves R.W. (2012). Broadband simulation plan for analysis of footwall / hanging-wall and rupture directivity effects, personal correspondence.

Graves, R.W., Pitarka A. (2010), Broadband ground motion simulation using hybrid approach, *Bulletin of Seismological Society of America. Bull. Seism. Soc. Am.*, **100**, 5A, 2095-2123.

Idriss I.M. (2008). An NGA empirical model for estimating the horizontal spectral values generated by shallow crustal earthquakes, *Earthq. Spectra*, 24(1): 217–242.

Idriss I.M. (2013). NGA-West2 model for estimating average horizontal values of pseudo-absolute spectral accelerations generated by crustal earthquakes. *Report PEER 2013/0*8 Pacific Earthquake Engineering Research Center, University of California, Berkeley, CA.

PEER (2005). Metadata used in the PEER Lifelines Next Generation Attenuation project for the development of the NGA flatfile, Pacific Earthquake Engineering Research Center, University of California, Berkeley, CA., http://peer.berkeley.edu/products/ngajprobect.html.

PEER REPORTS

PEER reports are available as a free PDF download from http://peer.berkeley.edu/publications/peer_reports_complete.html. Printed hard copies of PEER reports can be ordered directly from our printer by following the instructions at http://peer.berkeley.edu/publications/peer_reports.html. For other related questions about the PEER Report Series, contact the Pacific Earthquake Engineering Research Center, 325 Davis Hall mail code 1792, Berkeley, CA 94720. Tel.: (510) 642-3437; Fax: (510) 665-1655; Email: peer_editor@berkeley.edu

PEER 2013/21 *Seismic Design and Performance of Bridges with Columns on Rocking Foundations.* Grigorios Antonellis and Marios Panagiotou. September 2013.

PEER 2013/20 *Experimental and Analytical Studies on the Seismic Behavior of Conventional and Hybrid Braced Frames.* Jiun-Wei Lai and Stephen A. Mahin. September 2013.

PEER 2013/19 *Toward Resilient Communities: A Performance-Based Engineering Framework for Design and Evaluation of the Built Environment.* Michael William Mieler, Bozidar Stojadinovic, Robert J. Budnitz, Stephen A. Mahin and Mary C. Comerio. September 2013.

PEER 2013/18 *Identification of Site Parameters that Improve Predictions of Site Amplification.* Ellen M. Rathje and Sara Navidi. July 2013.

PEER 2013/17 *Response Spectrum Analysis of Concrete Gravity Dams Including Dam-Water-Foundation Interaction.* Arnkjell Løkke and Anil K. Chopra. July 2013.

PEER 2013/16 *Effect of hoop reinforcement spacing on the cyclic response of large reinforced concrete special moment frame beams.* Marios Panagiotou, Tea Visnjic, Grigorios Antonellis, Panagiotis Galanis, and Jack P. Moehle. June 2013.

PEER 2013/15 *publication pending*

PEER 2013/14 *Hanging-Wall Scaling using Finite-Fault Simulations.* Jennifer L. Donahue and Norman A. Abrahamson. September 2013.

PEER 2013/13 *publication pending*

PEER 2013/12 *Nonlinear Horizontal Site Response for the NGA-West2 Project.* Ronnie Kamai, Norman A. Abramson, Walter J. Silva. May 2013.

PEER 2013/11 *Epistemic Uncertainty for NGA-West2 Models.* Linda Al Atik and Robert R. Youngs. May 2013.

PEER 2013/10 *NGA-West 2 Models for Ground-Motion Directionality.* Shrey K. Shahi and Jack W. Baker. May 2013.

PEER 2013/09 *Final Report of the NGA-West2 Directivity Working Group.* Paul Spudich, Jeffrey R. Bayless, Jack W. Baker, Brian S.J. Chiou, Badie Rowshandel, Shrey Shahi, and Paul Somerville. May 2013.

PEER 2013/08 *NGA-West2 Model for Estimating Average Horizontal Values of Pseudo-Absolute Spectral Accelerations Generated by Crustal Earthquakes.* I. M. Idriss. May 2013.

PEER 2013/07 *Update of the Chiou and Youngs NGA Ground Motion Model for Average Horizontal Component of Peak Ground Motion and Response Spectra.* Brian Chiou and Robert Youngs. May 2013.

PEER 2013/06 *NGA-West2 Campbell-Bozorgnia Ground Motion Model for the Horizontal Components of PGA, PGV, and 5%-Damped Elastic Pseudo-Acceleration Response Spectra for Periods Ranging from 0.01 to 10 sec.* Kenneth W. Campbell and Yousef Bozorgnia. May 2013.

PEER 2013/05 *NGA-West 2 Equations for Predicting Response Spectral Accelerations for Shallow Crustal Earthquakes.* David M. Boore, Jonathan P. Stewart, Emel Seyhan, Gail M. Atkinson. May 2013.

PEER 2013/04 *Update of the AS08 Ground-Motion Prediction Equations Based on the NGA-West2 Data Set.* Norman Abrahamson, Walter Silva, and Ronnie Kamai. May 2013.

PEER 2013/03 *PEER NGA-West2 Database.* Timothy D. Ancheta, Robert B. Darragh, Jonathan P. Stewart, Emel Seyhan, Walter J. Silva, Brian S.J. Chiou, Katie E. Wooddell, Robert W. Graves, Albert R. Kottke, David M. Boore, Tadahiro Kishida, and Jennifer L. Donahue. May 2013.

PEER 2013/02 *Hybrid Simulation of the Seismic Response of Squat Reinforced Concrete Shear Walls.* Catherine A. Whyte and Bozidar Stojadinovic. May 2013.

PEER 2013/01 *Housing Recovery in Chile: A Qualitative Mid-program Review.* Mary C. Comerio. February 2013.

PEER 2012/08 *Guidelines for Estimation of Shear Wave Velocity.* Bernard R. Wair, Jason T. DeJong, and Thomas Shantz. December 2012.

PEER 2012/07 *Earthquake Engineering for Resilient Communities: 2012 PEER Internship Program Research Report Collection.* Heidi Tremayne (Editor), Stephen A. Mahin (Editor), Collin Anderson, Dustin Cook, Michael Erceg, Carlos Esparza, Jose Jimenez, Dorian Krausz, Andrew Lo, Stephanie Lopez, Nicole McCurdy, Paul Shipman, Alexander Strum, Eduardo Vega. December 2012.

PEER 2012/06 *Fragilities for Precarious Rocks at Yucca Mountain.* Matthew D. Purvance, Rasool Anooshehpoor, and James N. Brune. December 2012.

PEER 2012/05 *Development of Simplified Analysis Procedure for Piles in Laterally Spreading Layered Soils.* Christopher R. McGann, Pedro Arduino, and Peter Mackenzie–Helnwein. December 2012.

PEER 2012/04 *Unbonded Pre-Tensioned Columns for Bridges in Seismic Regions.* Phillip M. Davis, Todd M. Janes, Marc O. Eberhard, and John F. Stanton. December 2012.

PEER 2012/03 *Experimental and Analytical Studies on Reinforced Concrete Buildings with Seismically Vulnerable Beam-Column Joints.* Sangjoon Park and Khalid M. Mosalam. October 2012.

PEER 2012/02 *Seismic Performance of Reinforced Concrete Bridges Allowed to Uplift during Multi-Directional Excitation.* Andres Oscar Espinoza and Stephen A. Mahin. July 2012.

PEER 2012/01 *Spectral Damping Scaling Factors for Shallow Crustal Earthquakes in Active Tectonic Regions.* Sanaz Rezaeian, Yousef Bozorgnia, I. M. Idriss, Kenneth Campbell, Norman Abrahamson, and Walter Silva. July 2012.

PEER 2011/10 *Earthquake Engineering for Resilient Communities: 2011 PEER Internship Program Research Report Collection.* Eds. Heidi Faison and Stephen A. Mahin. December 2011.

PEER 2011/09 *Calibration of Semi-Stochastic Procedure for Simulating High-Frequency Ground Motions.* Jonathan P. Stewart, Emel Seyhan, and Robert W. Graves. December 2011.

PEER 2011/08 *Water Supply in regard to Fire Following Earthquake.* Charles Scawthorn. November 2011.

PEER 2011/07 *Seismic Risk Management in Urban Areas. Proceedings of a U.S.-Iran-Turkey Seismic Workshop.* September 2011.

PEER 2011/06 *The Use of Base Isolation Systems to Achieve Complex Seismic Performance Objectives.* Troy A. Morgan and Stephen A. Mahin. July 2011.

PEER 2011/05 *Case Studies of the Seismic Performance of Tall Buildings Designed by Alternative Means.* Task 12 Report for the Tall Buildings Initiative. Jack Moehle, Yousef Bozorgnia, Nirmal Jayaram, Pierson Jones, Mohsen Rahnama, Nilesh Shome, Zeynep Tuna, John Wallace, Tony Yang, and Farzin Zareian. July 2011.

PEER 2011/04 *Recommended Design Practice for Pile Foundations in Laterally Spreading Ground.* Scott A. Ashford, Ross W. Boulanger, and Scott J. Brandenberg. June 2011.

PEER 2011/03 *New Ground Motion Selection Procedures and Selected Motions for the PEER Transportation Research Program.* Jack W. Baker, Ting Lin, Shrey K. Shahi, and Nirmal Jayaram. March 2011.

PEER 2011/02 *A Bayesian Network Methodology for Infrastructure Seismic Risk Assessment and Decision Support.* Michelle T. Bensi, Armen Der Kiureghian, and Daniel Straub. March 2011.

PEER 2011/01 *Demand Fragility Surfaces for Bridges in Liquefied and Laterally Spreading Ground.* Scott J. Brandenberg, Jian Zhang, Pirooz Kashighandi, Yili Huo, and Minxing Zhao. March 2011.

PEER 2010/05 *Guidelines for Performance-Based Seismic Design of Tall Buildings.* Developed by the Tall Buildings Initiative. November 2010.

PEER 2010/04 *Application Guide for the Design of Flexible and Rigid Bus Connections between Substation Equipment Subjected to Earthquakes.* Jean-Bernard Dastous and Armen Der Kiureghian. September 2010.

PEER 2010/03 *Shear Wave Velocity as a Statistical Function of Standard Penetration Test Resistance and Vertical Effective Stress at Caltrans Bridge Sites.* Scott J. Brandenberg, Naresh Bellana, and Thomas Shantz. June 2010.

PEER 2010/02 *Stochastic Modeling and Simulation of Ground Motions for Performance-Based Earthquake Engineering.* Sanaz Rezaeian and Armen Der Kiureghian. June 2010.

PEER 2010/01 *Structural Response and Cost Characterization of Bridge Construction Using Seismic Performance Enhancement Strategies.* Ady Aviram, Božidar Stojadinović, Gustavo J. Parra-Montesinos, and Kevin R. Mackie. March 2010.

PEER 2009/03 *The Integration of Experimental and Simulation Data in the Study of Reinforced Concrete Bridge Systems Including Soil-Foundation-Structure Interaction.* Matthew Dryden and Gregory L. Fenves. November 2009.

PEER 2009/02 *Improving Earthquake Mitigation through Innovations and Applications in Seismic Science, Engineering, Communication, and Response. Proceedings of a U.S.-Iran Seismic Workshop.* October 2009.

PEER 2009/01 *Evaluation of Ground Motion Selection and Modification Methods: Predicting Median Interstory Drift Response of Buildings.* Curt B. Haselton, Ed. June 2009.

PEER 2008/10 *Technical Manual for Strata.* Albert R. Kottke and Ellen M. Rathje. February 2009.

PEER 2008/09 *NGA Model for Average Horizontal Component of Peak Ground Motion and Response Spectra.* Brian S.-J. Chiou and Robert R. Youngs. November 2008.

PEER 2008/08 *Toward Earthquake-Resistant Design of Concentrically Braced Steel Structures.* Patxi Uriz and Stephen A. Mahin. November 2008.

PEER 2008/07 *Using OpenSees for Performance-Based Evaluation of Bridges on Liquefiable Soils.* Stephen L. Kramer, Pedro Arduino, and HyungSuk Shin. November 2008.

PEER 2008/06 *Shaking Table Tests and Numerical Investigation of Self-Centering Reinforced Concrete Bridge Columns.* Hyung IL Jeong, Junichi Sakai, and Stephen A. Mahin. September 2008.

PEER 2008/05 *Performance-Based Earthquake Engineering Design Evaluation Procedure for Bridge Foundations Undergoing Liquefaction-Induced Lateral Ground Displacement.* Christian A. Ledezma and Jonathan D. Bray. August 2008.

PEER 2008/04 *Benchmarking of Nonlinear Geotechnical Ground Response Analysis Procedures.* Jonathan P. Stewart, Annie On-Lei Kwok, Yousseff M. A. Hashash, Neven Matasovic, Robert Pyke, Zhiliang Wang, and Zhaohui Yang. August 2008.

PEER 2008/03 *Guidelines for Nonlinear Analysis of Bridge Structures in California.* Ady Aviram, Kevin R. Mackie, and Božidar Stojadinović. August 2008.

PEER 2008/02 *Treatment of Uncertainties in Seismic-Risk Analysis of Transportation Systems.* Evangelos Stergiou and Anne S. Kiremidjian. July 2008.

PEER 2008/01 *Seismic Performance Objectives for Tall Buildings.* William T. Holmes, Charles Kircher, William Petak, and Nabih Youssef. August 2008.

PEER 2007/12 *An Assessment to Benchmark the Seismic Performance of a Code-Conforming Reinforced Concrete Moment-Frame Building.* Curt Haselton, Christine A. Goulet, Judith Mitrani-Reiser, James L. Beck, Gregory G. Deierlein, Keith A. Porter, Jonathan P. Stewart, and Ertugrul Taciroglu. August 2008.

PEER 2007/11 *Bar Buckling in Reinforced Concrete Bridge Columns.* Wayne A. Brown, Dawn E. Lehman, and John F. Stanton. February 2008.

PEER 2007/10 *Computational Modeling of Progressive Collapse in Reinforced Concrete Frame Structures.* Mohamed M. Talaat and Khalid M. Mosalam. May 2008.

PEER 2007/09 *Integrated Probabilistic Performance-Based Evaluation of Benchmark Reinforced Concrete Bridges.* Kevin R. Mackie, John-Michael Wong, and Božidar Stojadinović. January 2008.

PEER 2007/08 *Assessing Seismic Collapse Safety of Modern Reinforced Concrete Moment-Frame Buildings.* Curt B. Haselton and Gregory G. Deierlein. February 2008.

PEER 2007/07 *Performance Modeling Strategies for Modern Reinforced Concrete Bridge Columns.* Michael P. Berry and Marc O. Eberhard. April 2008.

PEER 2007/06 *Development of Improved Procedures for Seismic Design of Buried and Partially Buried Structures.* Linda Al Atik and Nicholas Sitar. June 2007.

PEER 2007/05 *Uncertainty and Correlation in Seismic Risk Assessment of Transportation Systems.* Renee G. Lee and Anne S. Kiremidjian. July 2007.

PEER 2007/04 *Numerical Models for Analysis and Performance-Based Design of Shallow Foundations Subjected to Seismic Loading.* Sivapalan Gajan, Tara C. Hutchinson, Bruce L. Kutter, Prishati Raychowdhury, José A. Ugalde, and Jonathan P. Stewart. May 2008.

PEER 2007/03 *Beam-Column Element Model Calibrated for Predicting Flexural Response Leading to Global Collapse of RC Frame Buildings.* Curt B. Haselton, Abbie B. Liel, Sarah Taylor Lange, and Gregory G. Deierlein. May 2008.

PEER 2007/02 *Campbell-Bozorgnia NGA Ground Motion Relations for the Geometric Mean Horizontal Component of Peak and Spectral Ground Motion Parameters.* Kenneth W. Campbell and Yousef Bozorgnia. May 2007.

PEER 2007/01 *Boore-Atkinson NGA Ground Motion Relations for the Geometric Mean Horizontal Component of Peak and Spectral Ground Motion Parameters.* David M. Boore and Gail M. Atkinson. May. May 2007.

PEER 2006/12 *Societal Implications of Performance-Based Earthquake Engineering.* Peter J. May. May 2007.

PEER 2006/11 *Probabilistic Seismic Demand Analysis Using Advanced Ground Motion Intensity Measures, Attenuation Relationships, and Near-Fault Effects.* Polsak Tothong and C. Allin Cornell. March 2007.

PEER 2006/10 *Application of the PEER PBEE Methodology to the I-880 Viaduct.* Sashi Kunnath. February 2007.

PEER 2006/09 *Quantifying Economic Losses from Travel Forgone Following a Large Metropolitan Earthquake.* James Moore, Sungbin Cho, Yue Yue Fan, and Stuart Werner. November 2006.

PEER 2006/08 *Vector-Valued Ground Motion Intensity Measures for Probabilistic Seismic Demand Analysis.* Jack W. Baker and C. Allin Cornell. October 2006.

PEER 2006/07 *Analytical Modeling of Reinforced Concrete Walls for Predicting Flexural and Coupled–Shear-Flexural Responses.* Kutay Orakcal, Leonardo M. Massone, and John W. Wallace. October 2006.

PEER 2006/06 *Nonlinear Analysis of a Soil-Drilled Pier System under Static and Dynamic Axial Loading.* Gang Wang and Nicholas Sitar. November 2006.

PEER 2006/05 *Advanced Seismic Assessment Guidelines.* Paolo Bazzurro, C. Allin Cornell, Charles Menun, Maziar Motahari, and Nicolas Luco. September 2006.

PEER 2006/04 *Probabilistic Seismic Evaluation of Reinforced Concrete Structural Components and Systems.* Tae Hyung Lee and Khalid M. Mosalam. August 2006.

PEER 2006/03 *Performance of Lifelines Subjected to Lateral Spreading.* Scott A. Ashford and Teerawut Juirnarongrit. July 2006.

PEER 2006/02 *Pacific Earthquake Engineering Research Center Highway Demonstration Project.* Anne Kiremidjian, James Moore, Yue Yue Fan, Nesrin Basoz, Ozgur Yazali, and Meredith Williams. April 2006.

PEER 2006/01 *Bracing Berkeley. A Guide to Seismic Safety on the UC Berkeley Campus.* Mary C. Comerio, Stephen Tobriner, and Ariane Fehrenkamp. January 2006.

PEER 2005/16 *Seismic Response and Reliability of Electrical Substation Equipment and Systems.* Junho Song, Armen Der Kiureghian, and Jerome L. Sackman. April 2006.

PEER 2005/15 *CPT-Based Probabilistic Assessment of Seismic Soil Liquefaction Initiation.* R. E. S. Moss, R. B. Seed, R. E. Kayen, J. P. Stewart, and A. Der Kiureghian. April 2006.

PEER 2005/14 *Workshop on Modeling of Nonlinear Cyclic Load-Deformation Behavior of Shallow Foundations.* Bruce L. Kutter, Geoffrey Martin, Tara Hutchinson, Chad Harden, Sivapalan Gajan, and Justin Phalen. March 2006.

PEER 2005/13 *Stochastic Characterization and Decision Bases under Time-Dependent Aftershock Risk in Performance-Based Earthquake Engineering.* Gee Liek Yeo and C. Allin Cornell. July 2005.

PEER 2005/12 *PEER Testbed Study on a Laboratory Building: Exercising Seismic Performance Assessment.* Mary C. Comerio, editor. November 2005.

PEER 2005/11 *Van Nuys Hotel Building Testbed Report: Exercising Seismic Performance Assessment.* Helmut Krawinkler, editor. October 2005.

PEER 2005/10 *First NEES/E-Defense Workshop on Collapse Simulation of Reinforced Concrete Building Structures.* September 2005.

PEER 2005/09 *Test Applications of Advanced Seismic Assessment Guidelines.* Joe Maffei, Karl Telleen, Danya Mohr, William Holmes, and Yuki Nakayama. August 2006.

PEER 2005/08 *Damage Accumulation in Lightly Confined Reinforced Concrete Bridge Columns.* R. Tyler Ranf, Jared M. Nelson, Zach Price, Marc O. Eberhard, and John F. Stanton. April 2006.

PEER 2005/07 *Experimental and Analytical Studies on the Seismic Response of Freestanding and Anchored Laboratory Equipment.* Dimitrios Konstantinidis and Nicos Makris. January 2005.

PEER 2005/06 *Global Collapse of Frame Structures under Seismic Excitations.* Luis F. Ibarra and Helmut Krawinkler. September 2005.

PEER 2005//05 *Performance Characterization of Bench- and Shelf-Mounted Equipment.* Samit Ray Chaudhuri and Tara C. Hutchinson. May 2006.

PEER 2005/04 *Numerical Modeling of the Nonlinear Cyclic Response of Shallow Foundations.* Chad Harden, Tara Hutchinson, Geoffrey R. Martin, and Bruce L. Kutter. August 2005.

PEER 2005/03 *A Taxonomy of Building Components for Performance-Based Earthquake Engineering.* Keith A. Porter. September 2005.

PEER 2005/02 *Fragility Basis for California Highway Overpass Bridge Seismic Decision Making.* Kevin R. Mackie and Božidar Stojadinović. June 2005.

PEER 2005/01 *Empirical Characterization of Site Conditions on Strong Ground Motion.* Jonathan P. Stewart, Yoojoong Choi, and Robert W. Graves. June 2005.

PEER 2004/09 *Electrical Substation Equipment Interaction: Experimental Rigid Conductor Studies.* Christopher Stearns and André Filiatrault. February 2005.

PEER 2004/08 *Seismic Qualification and Fragility Testing of Line Break 550-kV Disconnect Switches.* Shakhzod M. Takhirov, Gregory L. Fenves, and Eric Fujisaki. January 2005.

PEER 2004/07 *Ground Motions for Earthquake Simulator Qualification of Electrical Substation Equipment.* Shakhzod M. Takhirov, Gregory L. Fenves, Eric Fujisaki, and Don Clyde. January 2005.

PEER 2004/06 *Performance-Based Regulation and Regulatory Regimes.* Peter J. May and Chris Koski. September 2004.

PEER 2004/05 *Performance-Based Seismic Design Concepts and Implementation: Proceedings of an International Workshop.* Peter Fajfar and Helmut Krawinkler, editors. September 2004.

PEER 2004/04 *Seismic Performance of an Instrumented Tilt-up Wall Building.* James C. Anderson and Vitelmo V. Bertero. July 2004.

PEER 2004/03 *Evaluation and Application of Concrete Tilt-up Assessment Methodologies.* Timothy Graf and James O. Malley. October 2004.

PEER 2004/02 *Analytical Investigations of New Methods for Reducing Residual Displacements of Reinforced Concrete Bridge Columns.* Junichi Sakai and Stephen A. Mahin. August 2004.

PEER 2004/01 *Seismic Performance of Masonry Buildings and Design Implications.* Kerri Anne Taeko Tokoro, James C. Anderson, and Vitelmo V. Bertero. February 2004.

PEER 2003/18 *Performance Models for Flexural Damage in Reinforced Concrete Columns.* Michael Berry and Marc Eberhard. August 2003.

PEER 2003/17 *Predicting Earthquake Damage in Older Reinforced Concrete Beam-Column Joints.* Catherine Pagni and Laura Lowes. October 2004.

PEER 2003/16 *Seismic Demands for Performance-Based Design of Bridges.* Kevin Mackie and Božidar Stojadinović. August 2003.

PEER 2003/15 *Seismic Demands for Nondeteriorating Frame Structures and Their Dependence on Ground Motions.* Ricardo Antonio Medina and Helmut Krawinkler. May 2004.

PEER 2003/14 *Finite Element Reliability and Sensitivity Methods for Performance-Based Earthquake Engineering.* Terje Haukaas and Armen Der Kiureghian. April 2004.

PEER 2003/13 *Effects of Connection Hysteretic Degradation on the Seismic Behavior of Steel Moment-Resisting Frames.* Janise E. Rodgers and Stephen A. Mahin. March 2004.

PEER 2003/12 *Implementation Manual for the Seismic Protection of Laboratory Contents: Format and Case Studies.* William T. Holmes and Mary C. Comerio. October 2003.

PEER 2003/11 *Fifth U.S.-Japan Workshop on Performance-Based Earthquake Engineering Methodology for Reinforced Concrete Building Structures.* February 2004.

PEER 2003/10 *A Beam-Column Joint Model for Simulating the Earthquake Response of Reinforced Concrete Frames.* Laura N. Lowes, Nilanjan Mitra, and Arash Altoontash. February 2004.

PEER 2003/09 *Sequencing Repairs after an Earthquake: An Economic Approach.* Marco Casari and Simon J. Wilkie. April 2004.

PEER 2003/08 *A Technical Framework for Probability-Based Demand and Capacity Factor Design (DCFD) Seismic Formats*. Fatemeh Jalayer and C. Allin Cornell. November 2003.

PEER 2003/07 *Uncertainty Specification and Propagation for Loss Estimation Using FOSM Methods.* Jack W. Baker and C. Allin Cornell. September 2003.

PEER 2003/06 *Performance of Circular Reinforced Concrete Bridge Columns under Bidirectional Earthquake Loading*. Mahmoud M. Hachem, Stephen A. Mahin, and Jack P. Moehle. February 2003.

PEER 2003/05 *Response Assessment for Building-Specific Loss Estimation.* Eduardo Miranda and Shahram Taghavi. September 2003.

PEER 2003/04 *Experimental Assessment of Columns with Short Lap Splices Subjected to Cyclic Loads*. Murat Melek, John W. Wallace, and Joel Conte. April 2003.

PEER 2003/03 *Probabilistic Response Assessment for Building-Specific Loss Estimation.* Eduardo Miranda and Hesameddin Aslani. September 2003.

PEER 2003/02 *Software Framework for Collaborative Development of Nonlinear Dynamic Analysis Program.* Jun Peng and Kincho H. Law. September 2003.

PEER 2003/01 *Shake Table Tests and Analytical Studies on the Gravity Load Collapse of Reinforced Concrete Frames.* Kenneth John Elwood and Jack P. Moehle. November 2003.

PEER 2002/24 *Performance of Beam to Column Bridge Joints Subjected to a Large Velocity Pulse.* Natalie Gibson, André Filiatrault, and Scott A. Ashford. April 2002.

PEER 2002/23 *Effects of Large Velocity Pulses on Reinforced Concrete Bridge Columns.* Greg L. Orozco and Scott A. Ashford. April 2002.

PEER 2002/22 *Characterization of Large Velocity Pulses for Laboratory Testing.* Kenneth E. Cox and Scott A. Ashford. April 2002.

PEER 2002/21 *Fourth U.S.-Japan Workshop on Performance-Based Earthquake Engineering Methodology for Reinforced Concrete Building Structures.* December 2002.

PEER 2002/20 *Barriers to Adoption and Implementation of PBEE Innovations.* Peter J. May. August 2002.

PEER 2002/19 *Economic-Engineered Integrated Models for Earthquakes: Socioeconomic Impacts.* Peter Gordon, James E. Moore II, and Harry W. Richardson. July 2002.

PEER 2002/18 *Assessment of Reinforced Concrete Building Exterior Joints with Substandard Details.* Chris P. Pantelides, Jon Hansen, Justin Nadauld, and Lawrence D. Reaveley. May 2002.

PEER 2002/17 *Structural Characterization and Seismic Response Analysis of a Highway Overcrossing Equipped with Elastomeric Bearings and Fluid Dampers: A Case Study.* Nicos Makris and Jian Zhang. November 2002.

PEER 2002/16 *Estimation of Uncertainty in Geotechnical Properties for Performance-Based Earthquake Engineering.* Allen L. Jones, Steven L. Kramer, and Pedro Arduino. December 2002.

PEER 2002/15 *Seismic Behavior of Bridge Columns Subjected to Various Loading Patterns.* Asadollah Esmaeily-Gh. and Yan Xiao. December 2002.

PEER 2002/14 *Inelastic Seismic Response of Extended Pile Shaft Supported Bridge Structures.* T.C. Hutchinson, R.W. Boulanger, Y.H. Chai, and I.M. Idriss. December 2002.

PEER 2002/13 *Probabilistic Models and Fragility Estimates for Bridge Components and Systems.* Paolo Gardoni, Armen Der Kiureghian, and Khalid M. Mosalam. June 2002.

PEER 2002/12 *Effects of Fault Dip and Slip Rake on Near-Source Ground Motions: Why Chi-Chi Was a Relatively Mild M7.6 Earthquake.* Brad T. Aagaard, John F. Hall, and Thomas H. Heaton. December 2002.

PEER 2002/11 *Analytical and Experimental Study of Fiber-Reinforced Strip Isolators*. James M. Kelly and Shakhzod M. Takhirov. September 2002.

PEER 2002/10 *Centrifuge Modeling of Settlement and Lateral Spreading with Comparisons to Numerical Analyses***.** Sivapalan Gajan and Bruce L. Kutter. January 2003.

PEER 2002/09 *Documentation and Analysis of Field Case Histories of Seismic Compression during the 1994 Northridge, California, Earthquake.* Jonathan P. Stewart, Patrick M. Smith, Daniel H. Whang, and Jonathan D. Bray. October 2002.

PEER 2002/08 *Component Testing, Stability Analysis and Characterization of Buckling-Restrained Unbonded Braces™.* Cameron Black, Nicos Makris, and Ian Aiken. September 2002.

PEER 2002/07 *Seismic Performance of Pile-Wharf Connections.* Charles W. Roeder, Robert Graff, Jennifer Soderstrom, and Jun Han Yoo. December 2001.

PEER 2002/06 *The Use of Benefit-Cost Analysis for Evaluation of Performance-Based Earthquake Engineering Decisions.* Richard O. Zerbe and Anthony Falit-Baiamonte. September 2001.

PEER 2002/05 *Guidelines, Specifications, and Seismic Performance Characterization of Nonstructural Building Components and Equipment*. André Filiatrault, Constantin Christopoulos, and Christopher Stearns. September 2001.

PEER 2002/04 *Consortium of Organizations for Strong-Motion Observation Systems and the Pacific Earthquake Engineering Research Center Lifelines Program: Invited Workshop on Archiving and Web Dissemination of Geotechnical Data, 4–5 October 2001*. September 2002.

PEER 2002/03 *Investigation of Sensitivity of Building Loss Estimates to Major Uncertain Variables for the Van Nuys Testbed.* Keith A. Porter, James L. Beck, and Rustem V. Shaikhutdinov. August 2002.

PEER 2002/02 *The Third U.S.-Japan Workshop on Performance-Based Earthquake Engineering Methodology for Reinforced Concrete Building Structures.* July 2002.

PEER 2002/01 *Nonstructural Loss Estimation: The UC Berkeley Case Study.* Mary C. Comerio and John C. Stallmeyer. December 2001.

PEER 2001/16 *Statistics of SDF-System Estimate of Roof Displacement for Pushover Analysis of Buildings.* Anil K. Chopra, Rakesh K. Goel, and Chatpan Chintanapakdee. December 2001.

PEER 2001/15 *Damage to Bridges during the 2001 Nisqually Earthquake.* R. Tyler Ranf, Marc O. Eberhard, and Michael P. Berry. November 2001.

PEER 2001/14 *Rocking Response of Equipment Anchored to a Base Foundation.* Nicos Makris and Cameron J. Black. September 2001.

PEER 2001/13 *Modeling Soil Liquefaction Hazards for Performance-Based Earthquake Engineering.* Steven L. Kramer and Ahmed-W. Elgamal. February 2001.

PEER 2001/12 *Development of Geotechnical Capabilities in OpenSees.* Boris Jeremić. September 2001.

PEER 2001/11 *Analytical and Experimental Study of Fiber-Reinforced Elastomeric Isolators*. James M. Kelly and Shakhzod M. Takhirov. September 2001.

PEER 2001/10 *Amplification Factors for Spectral Acceleration in Active Regions.* Jonathan P. Stewart, Andrew H. Liu, Yoojoong Choi, and Mehmet B. Baturay. December 2001.

PEER 2001/09 *Ground Motion Evaluation Procedures for Performance-Based Design.* Jonathan P. Stewart, Shyh-Jeng Chiou, Jonathan D. Bray, Robert W. Graves, Paul G. Somerville, and Norman A. Abrahamson. September 2001.

PEER 2001/08 *Experimental and Computational Evaluation of Reinforced Concrete Bridge Beam-Column Connections for Seismic Performance*. Clay J. Naito, Jack P. Moehle, and Khalid M. Mosalam. November 2001.

PEER 2001/07 *The Rocking Spectrum and the Shortcomings of Design Guidelines.* Nicos Makris and Dimitrios Konstantinidis. August 2001.

PEER 2001/06 *Development of an Electrical Substation Equipment Performance Database for Evaluation of Equipment Fragilities*. Thalia Agnanos. April 1999.

PEER 2001/05 *Stiffness Analysis of Fiber-Reinforced Elastomeric Isolators*. Hsiang-Chuan Tsai and James M. Kelly. May 2001.

PEER 2001/04 *Organizational and Societal Considerations for Performance-Based Earthquake Engineering.* Peter J. May. April 2001.

PEER 2001/03 *A Modal Pushover Analysis Procedure to Estimate Seismic Demands for Buildings: Theory and Preliminary Evaluation.* Anil K. Chopra and Rakesh K. Goel. January 2001.

PEER 2001/02 *Seismic Response Analysis of Highway Overcrossings Including Soil-Structure Interaction.* Jian Zhang and Nicos Makris. March 2001.

PEER 2001/01 *Experimental Study of Large Seismic Steel Beam-to-Column Connections.* Egor P. Popov and Shakhzod M. Takhirov. November 2000.

PEER 2000/10 *The Second U.S.-Japan Workshop on Performance-Based Earthquake Engineering Methodology for Reinforced Concrete Building Structures.* March 2000.

PEER 2000/09 *Structural Engineering Reconnaissance of the August 17, 1999 Earthquake: Kocaeli (Izmit), Turkey.* Halil Sezen, Kenneth J. Elwood, Andrew S. Whittaker, Khalid Mosalam, John J. Wallace, and John F. Stanton. December 2000.

PEER 2000/08 *Behavior of Reinforced Concrete Bridge Columns Having Varying Aspect Ratios and Varying Lengths of Confinement.* Anthony J. Calderone, Dawn E. Lehman, and Jack P. Moehle. January 2001.

PEER 2000/07 *Cover-Plate and Flange-Plate Reinforced Steel Moment-Resisting Connections.* Taejin Kim, Andrew S. Whittaker, Amir S. Gilani, Vitelmo V. Bertero, and Shakhzod M. Takhirov. September 2000.

PEER 2000/06 *Seismic Evaluation and Analysis of 230-kV Disconnect Switches.* Amir S. J. Gilani, Andrew S. Whittaker, Gregory L. Fenves, Chun-Hao Chen, Henry Ho, and Eric Fujisaki. July 2000.

PEER 2000/05 *Performance-Based Evaluation of Exterior Reinforced Concrete Building Joints for Seismic Excitation.* Chandra Clyde, Chris P. Pantelides, and Lawrence D. Reaveley. July 2000.

PEER 2000/04 *An Evaluation of Seismic Energy Demand: An Attenuation Approach.* Chung-Che Chou and Chia-Ming Uang. July 1999.

PEER 2000/03 *Framing Earthquake Retrofitting Decisions: The Case of Hillside Homes in Los Angeles.* Detlof von Winterfeldt, Nels Roselund, and Alicia Kitsuse. March 2000.

PEER 2000/02 *U.S.-Japan Workshop on the Effects of Near-Field Earthquake Shaking.* Andrew Whittaker, ed. July 2000.

PEER 2000/01 *Further Studies on Seismic Interaction in Interconnected Electrical Substation Equipment.* Armen Der Kiureghian, Kee-Jeung Hong, and Jerome L. Sackman. November 1999.

PEER 1999/14 *Seismic Evaluation and Retrofit of 230-kV Porcelain Transformer Bushings.* Amir S. Gilani, Andrew S. Whittaker, Gregory L. Fenves, and Eric Fujisaki. December 1999.

PEER 1999/13 *Building Vulnerability Studies: Modeling and Evaluation of Tilt-up and Steel Reinforced Concrete Buildings.* John W. Wallace, Jonathan P. Stewart, and Andrew S. Whittaker, editors. December 1999.

PEER 1999/12 *Rehabilitation of Nonductile RC Frame Building Using Encasement Plates and Energy-Dissipating Devices.* Mehrdad Sasani, Vitelmo V. Bertero, James C. Anderson. December 1999.

PEER 1999/11 *Performance Evaluation Database for Concrete Bridge Components and Systems under Simulated Seismic Loads.* Yael D. Hose and Frieder Seible. November 1999.

PEER 1999/10 *U.S.-Japan Workshop on Performance-Based Earthquake Engineering Methodology for Reinforced Concrete Building Structures.* December 1999.

PEER 1999/09 *Performance Improvement of Long Period Building Structures Subjected to Severe Pulse-Type Ground Motions.* James C. Anderson, Vitelmo V. Bertero, and Raul Bertero. October 1999.

PEER 1999/08 *Envelopes for Seismic Response Vectors.* Charles Menun and Armen Der Kiureghian. July 1999.

PEER 1999/07 *Documentation of Strengths and Weaknesses of Current Computer Analysis Methods for Seismic Performance of Reinforced Concrete Members.* William F. Cofer. November 1999.

PEER 1999/06 *Rocking Response and Overturning of Anchored Equipment under Seismic Excitations.* Nicos Makris and Jian Zhang. November 1999.

PEER 1999/05 *Seismic Evaluation of 550 kV Porcelain Transformer Bushings.* Amir S. Gilani, Andrew S. Whittaker, Gregory L. Fenves, and Eric Fujisaki. October 1999.

PEER 1999/04 *Adoption and Enforcement of Earthquake Risk-Reduction Measures.* Peter J. May, Raymond J. Burby, T. Jens Feeley, and Robert Wood.

PEER 1999/03 *Task 3 Characterization of Site Response General Site Categories.* Adrian Rodriguez-Marek, Jonathan D. Bray, and Norman Abrahamson. February 1999.

PEER 1999/02 *Capacity-Demand-Diagram Methods for Estimating Seismic Deformation of Inelastic Structures: SDF Systems.* Anil K. Chopra and Rakesh Goel. April 1999.

PEER 1999/01 *Interaction in Interconnected Electrical Substation Equipment Subjected to Earthquake Ground Motions.* Armen Der Kiureghian, Jerome L. Sackman, and Kee-Jeung Hong. February 1999.

PEER 1998/08 *Behavior and Failure Analysis of a Multiple-Frame Highway Bridge in the 1994 Northridge Earthquake.* Gregory L. Fenves and Michael Ellery. December 1998.

PEER 1998/07 *Empirical Evaluation of Inertial Soil-Structure Interaction Effects.* Jonathan P. Stewart, Raymond B. Seed, and Gregory L. Fenves. November 1998.

PEER 1998/06 *Effect of Damping Mechanisms on the Response of Seismic Isolated Structures.* Nicos Makris and Shih-Po Chang. November 1998.

PEER 1998/05 *Rocking Response and Overturning of Equipment under Horizontal Pulse-Type Motions.* Nicos Makris and Yiannis Roussos. October 1998.

PEER 1998/04 *Pacific Earthquake Engineering Research Invitational Workshop Proceedings, May 14–15, 1998: Defining the Links between Planning, Policy Analysis, Economics and Earthquake Engineering.* Mary Comerio and Peter Gordon. September 1998.

PEER 1998/03 *Repair/Upgrade Procedures for Welded Beam to Column Connections.* James C. Anderson and Xiaojing Duan. May 1998.

PEER 1998/02 *Seismic Evaluation of 196 kV Porcelain Transformer Bushings.* Amir S. Gilani, Juan W. Chavez, Gregory L. Fenves, and Andrew S. Whittaker. May 1998.

PEER 1998/01 *Seismic Performance of Well-Confined Concrete Bridge Columns.* Dawn E. Lehman and Jack P. Moehle. December 2000.

ONLINE PEER REPORTS

The following PEER reports are available by Internet only at http://peer.berkeley.edu/publications/peer_reports_complete.html.

PEER 2012/103 *Performance-Based Seismic Demand Assessment of Concentrically Braced Steel Frame Buildings.* Chui-Hsin Chen and Stephen A. Mahin. December 2012.

PEER 2012/102 *Procedure to Restart an Interrupted Hybrid Simulation: Addendum to PEER Report 2010/103.* Vesna Terzic and Bozidar Stojadinovic. October 2012.

PEER 2012/101 *Mechanics of Fiber Reinforced Bearings.* James M. Kelly and Andrea Calabrese. February 2012.

PEER 2011/107 *Nonlinear Site Response and Seismic Compression at Vertical Array Strongly Shaken by 2007 Niigata-ken Chuetsu-oki Earthquake.* Eric Yee, Jonathan P. Stewart, and Kohji Tokimatsu. December 2011.

PEER 2011/106 *Self Compacting Hybrid Fiber Reinforced Concrete Composites for Bridge Columns.* Pardeep Kumar, Gabriel Jen, William Trono, Marios Panagiotou, and Claudia Ostertag. September 2011.

PEER 2011/105 *Stochastic Dynamic Analysis of Bridges Subjected to Spacially Varying Ground Motions.* Katerina Konakli and Armen Der Kiureghian. August 2011.

PEER 2011/104 *Design and Instrumentation of the 2010 E-Defense Four-Story Reinforced Concrete and Post-Tensioned Concrete Buildings.* Takuya Nagae, Kenichi Tahara, Taizo Matsumori, Hitoshi Shiohara, Toshimi Kabeyasawa, Susumu Kono, Minehiro Nishiyama (Japanese Research Team) and John Wallace, Wassim Ghannoum, Jack Moehle, Richard Sause, Wesley Keller, Zeynep Tuna (U.S. Research Team). June 2011.

PEER 2011/103 *In-Situ Monitoring of the Force Output of Fluid Dampers: Experimental Investigation.* Dimitrios Konstantinidis, James M. Kelly, and Nicos Makris. April 2011.

PEER 2011/102 *Ground-motion prediction equations 1964 - 2010.* John Douglas. April 2011.

PEER 2011/101 *Report of the Eighth Planning Meeting of NEES/E-Defense Collaborative Research on Earthquake Engineering.* Convened by the Hyogo Earthquake Engineering Research Center (NIED), NEES Consortium, Inc. February 2011.

PEER 2010/111 *Modeling and Acceptance Criteria for Seismic Design and Analysis of Tall Buildings.* Task 7 Report for the Tall Buildings Initiative - Published jointly by the Applied Technology Council. October 2010.

PEER 2010/110 *Seismic Performance Assessment and Probabilistic Repair Cost Analysis of Precast Concrete Cladding Systems for Multistory Buildlings.* Jeffrey P. Hunt and Božidar Stojadinovic. November 2010.

PEER 2010/109 *Report of the Seventh Joint Planning Meeting of NEES/E-Defense Collaboration on Earthquake Engineering. Held at the E-Defense, Miki, and Shin-Kobe, Japan, September 18–19, 2009.* August 2010.

PEER 2010/108 *Probabilistic Tsunami Hazard in California.* Hong Kie Thio, Paul Somerville, and Jascha Polet, preparers. October 2010.

PEER 2010/107 *Performance and Reliability of Exposed Column Base Plate Connections for Steel Moment-Resisting Frames.* Ady Aviram, Božidar Stojadinovic, and Armen Der Kiureghian. August 2010.

PEER 2010/106 *Verification of Probabilistic Seismic Hazard Analysis Computer Programs.* Patricia Thomas, Ivan Wong, and Norman Abrahamson. May 2010.

PEER 2010/105 *Structural Engineering Reconnaissance of the April 6, 2009, Abruzzo, Italy, Earthquake, and Lessons Learned.* M. Selim Günay and Khalid M. Mosalam. April 2010.

PEER 2010/104 *Simulating the Inelastic Seismic Behavior of Steel Braced Frames, Including the Effects of Low-Cycle Fatigue.* Yuli Huang and Stephen A. Mahin. April 2010.

PEER 2010/103 *Post-Earthquake Traffic Capacity of Modern Bridges in California.* Vesna Terzic and Božidar Stojadinović. March 2010.

PEER 2010/102 *Analysis of Cumulative Absolute Velocity (CAV) and JMA Instrumental Seismic Intensity (I_{JMA}) Using the PEER–NGA Strong Motion Database.* Kenneth W. Campbell and Yousef Bozorgnia. February 2010.

PEER 2010/101 *Rocking Response of Bridges on Shallow Foundations.* Jose A. Ugalde, Bruce L. Kutter, and Boris Jeremic. April 2010.

PEER 2009/109 *Simulation and Performance-Based Earthquake Engineering Assessment of Self-Centering Post-Tensioned Concrete Bridge Systems.* Won K. Lee and Sarah L. Billington. December 2009.

PEER 2009/108 *PEER Lifelines Geotechnical Virtual Data Center.* J. Carl Stepp, Daniel J. Ponti, Loren L. Turner, Jennifer N. Swift, Sean Devlin, Yang Zhu, Jean Benoit, and John Bobbitt. September 2009.

PEER 2009/107 *Experimental and Computational Evaluation of Current and Innovative In-Span Hinge Details in Reinforced Concrete Box-Girder Bridges: Part 2: Post-Test Analysis and Design Recommendations.* Matias A. Hube and Khalid M. Mosalam. December 2009.

PEER 2009/106 *Shear Strength Models of Exterior Beam-Column Joints without Transverse Reinforcement.* Sangjoon Park and Khalid M. Mosalam. November 2009.

PEER 2009/105 *Reduced Uncertainty of Ground Motion Prediction Equations through Bayesian Variance Analysis.* Robb Eric S. Moss. November 2009.

PEER 2009/104 *Advanced Implementation of Hybrid Simulation.* Andreas H. Schellenberg, Stephen A. Mahin, Gregory L. Fenves. November 2009.

PEER 2009/103 *Performance Evaluation of Innovative Steel Braced Frames.* T. Y. Yang, Jack P. Moehle, and Božidar Stojadinovic. August 2009.

PEER 2009/102 *Reinvestigation of Liquefaction and Nonliquefaction Case Histories from the 1976 Tangshan Earthquake.* Robb Eric Moss, Robert E. Kayen, Liyuan Tong, Songyu Liu, Guojun Cai, and Jiaer Wu. August 2009.

PEER 2009/101 *Report of the First Joint Planning Meeting for the Second Phase of NEES/E-Defense Collaborative Research on Earthquake Engineering.* Stephen A. Mahin et al. July 2009.

PEER 2008/104 *Experimental and Analytical Study of the Seismic Performance of Retaining Structures.* Linda Al Atik and Nicholas Sitar. January 2009.

PEER 2008/103 *Experimental and Computational Evaluation of Current and Innovative In-Span Hinge Details in Reinforced Concrete Box-Girder Bridges. Part 1: Experimental Findings and Pre-Test Analysis.* Matias A. Hube and Khalid M. Mosalam. January 2009.

PEER 2008/102 *Modeling of Unreinforced Masonry Infill Walls Considering In-Plane and Out-of-Plane Interaction.* Stephen Kadysiewski and Khalid M. Mosalam. January 2009.

PEER 2008/101 *Seismic Performance Objectives for Tall Buildings.* William T. Holmes, Charles Kircher, William Petak, and Nabih Youssef. August 2008.

PEER 2007/101 *Generalized Hybrid Simulation Framework for Structural Systems Subjected to Seismic Loading.* Tarek Elkhoraibi and Khalid M. Mosalam. July 2007.

PEER 2007/100 *Seismic Evaluation of Reinforced Concrete Buildings Including Effects of Masonry Infill Walls.* Alidad Hashemi and Khalid M. Mosalam. July 2007.

The Pacific Earthquake Engineering Research Center (PEER) is a multi-institutional research and education center with headquarters at the University of California, Berkeley. Investigators from over 20 universities, several consulting companies, and researchers at various state and federal government agencies contribute to research programs focused on performance-based earthquake engineering.

These research programs aim to identify and reduce the risks from major earthquakes to life safety and to the economy by including research in a wide variety of disciplines including structural and geotechnical engineering, geology/seismology, lifelines, transportation, architecture, economics, risk management, and public policy.

PEER is supported by federal, state, local, and regional agencies, together with industry partners.

PEER Core Institutions:
University of California, Berkeley (Lead Institution)
California Institute of Technology
Oregon State University
Stanford University
University of California, Davis
University of California, Irvine
University of California, Los Angeles
University of California, San Diego
University of Southern California
University of Washington

PEER reports can be ordered at http://peer.berkeley.edu/publications/peer_reports.html or by contacting

Pacific Earthquake Engineering Research Center
University of California, Berkeley
325 Davis Hall, mail code 1792
Berkeley, CA 94720-1792
Tel: 510-642-3437
Fax: 510-642-1655
Email: peer_editor@berkeley.edu

ISSN 1547-0587X